SSRG International Journal of Geo-informatics and Geological Science
ISSN: 2393–9206 / https://doi.org/10.14445/23939206/IJGGS-V10I1P101

Volume 10 Issue 1, 1-24, Jan-Apr 2023
© 2023 Seventh Sense Research Group®

Original Article

Application of Boreholes Redox Mapping Technique for Sandstone-Type Uranium Exploration in Arlit, Niger

Abdou Dodo Bohari[1,2,3], Ibrahim Sarki Laouali[1], Hamma Ada Moussa [1], Harouna Moussa[1], Nana Oumarou Diori[1]

[1]*Department of Geology Abdou Moumouni University, Niamey-Niger.*
[2]*Hohai University, Nanjing, China.*
[3]*GeoProbe Consult, Niamey-Niger.*

Received: 06 February 2023 Revised: 11 March 2023 Accepted: 22 March 2023 Published: 06 April 2023

Abstract *- Exploration is a key fundamental step in the process of any uranium mining activity. Moreover, a new deposit has been discovered in the context of mine development. The objective of the present research studies is to apply the borehole redox mapping technique as a guide for uranium exploration in the sedimentary environment. The Tarat formation in the study area is the Tarat formation in Arlit area is divided into four units (U4, U3, U2, and U1) such as Tarat Unit4 (U4) consists of reduced gray fine consolidated sandstone alternating clay-silt; Tarat Unit 3 (U3) is composed of coarse to medium sandstone with increasing presence of micro-conglomerate towards the bottom; Tarat Unit 2 (U2) characterized by reduced fine gray sandstone with kaolinitic cement and Tarat Unit 1 (U1) consists of coarse to micro-conglomerate gray sandstone. The results of oxyhydroxides distribution maps show high radiometric accumulation in low oxyhydroxides zones of the Tarat Unit (U4) and Tarat Unit (U3), while the Tarat Unit (U2) and Tarat Unit (U1) show less radiometric accumulation in high oxyhydroxides zones. Therefore, the generalized oxyhydroxide distribution maps of the whole Tarat Formation show that moderate to fewer oxidation zones are suitable for uranium mineralization. In contrast, zones with intense oxidation are poorly mineralized.*

Keywords *- Oxyhydroxide, Radiometry, Mineralization, Niger, Redox mapping.*

1. Introduction

Exploration for sandstones type Uranium in Niger started in the 1950s when the country was still under French colonial rule. The French Overseas Mining Bureau (BUMIFOM) discovered uranium showings in 1957 in the Agadez region [1-3]. The French Atomic Energy Agency (CEA) then started detailed exploration through airborne geophysical and ground geological surveys and drilling, leading to the discovery of several uranium deposits and their mining in the 1970s [1-5]. These activities decreased significantly due to the drop in uranium prices in the 80s.

The uranium exploration activities in Niger increased because of the high demand for uranium in 2006-2007. Niger has used this opportunity to deliver many uranium explorations licenses (all minerals included) [5]. There are two uranium-operating mining companies (COMINAK and SOMAIR) in Niger, and at the end of 2011, Niger got a third operating mining company (SOMINA) [5]. The sandstone-hosted uranium deposits in Tim-Mersoi basin, Niger, accumulated in the basin's upper Paleozoic sedimentary part (Carboniferous) and occur in medium to coarse-grained and stones deposited in a continental fluvial-deltaic sedimentary reducing environment of arid to humid climatic conditions rich in organic matter. The alteration from oxidized to a reduced environment is usually associated with oxide-hydroxide, pyrite, organic matter, and carbonate [8-15]. Recently, a new prospect with a potential uranium ore deposit has been identified within the basin, but in the current state of knowledge on uranium exploration, there is no well-documented literature about redox mapping during uranium exploration; hence the objective of this research study is therefore, to present the technique of borehole redox mapping during uranium exploration.

1.1. Location of the Study Area

The Tamari sector represents the prospect study area, mainly located on the east Tamou within SOMAÏR open-pit mining area. The study was carried out in the Arlit area from June to August 2018. It is between the WGS coordinates of 2072000 and 2075400mN, and between 322200 and 327200mE, limited to the East by the Harlequin sector, to the West by the Tamou deposits, to the South by the Tin-Adrar beam and to the North by the Arlette and Ariège deposits (Figure 1).

This is an open access article under the CC BY-NC-ND license (http://creativecommons.org/licenses/by-nc-nd/4.0/)

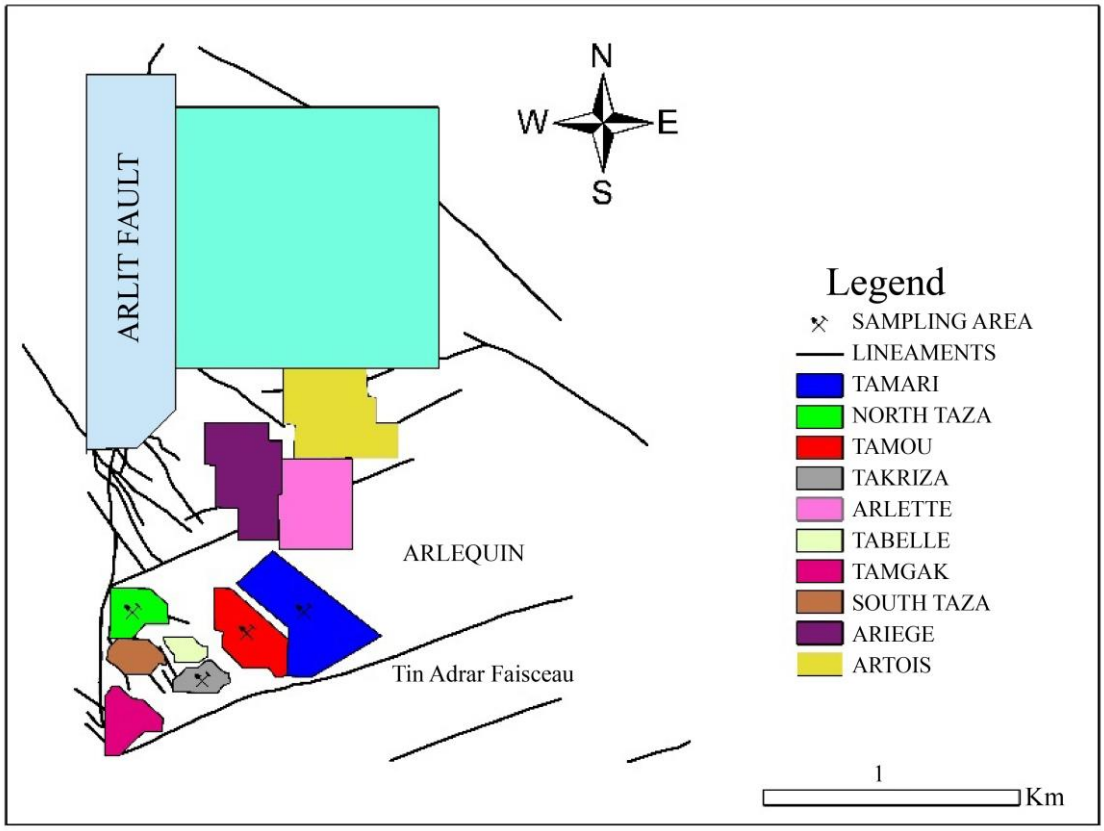

Fig. 1 Location of the study area within SOMAIR

1.2. Geological Setting

The Proterozoic basement of the Air massif and the intracratonic Tim Mersoi sedimentary basin dominates the geology of Niger. The crystalline basement formed during the Panafrican orogenesis consists of metamorphosed rocks, essentially metasediments, intruded by granites [3, 30]. Recognized lithologies include biotite gneiss, leptynitic gneiss and micaceous shale with quartzite and amphibolite. The granite intrusions are syntectonic, with the main phase of deformation occurring during the Panafrican orogenesis [3, 30].

The magmatic activity did continue with post-orogenesis granite intrusions during the Ordovician, Carboniferous and Jurassic. Volcanic activity also occurred during the Tertiary and Quaternary periods [17-19,30] (Figure 2). All of the uranium deposits from Niger are located in the Tim-Mersoï Basin, which covers 600 000 km2, half of the country's total area. The main deposits are located in the northern region of Arlit-Akouta and the southern regions of Madaouela, Imouraren and Azelik. The Tim Mersoï Basin is surrounded in the North by the Hoggar massif, on the West by the In-Guezzam ridge and in the East by the Aïr massif. To the South, the Tim Mersoï Basin extends to Iullemmeden Basin and Nigeria [8-9]. The stratigraphy of the eastern part of the Tim Mersoi basin is divided (from bottom to top) into four main sequences [3, 19-20] (Figure 3):

- The Lower Visean formations of the Terada Group consist of the coarse to conglomeratic sandstones of the Teragh and the marine clays of the Talak;
- The Upper Visean formations of the Tagora Group include two series starting with a fluvio- deltaic period, followed by a marine to epicontinental sedimentation and ending with a lacustre-alluvial period. The Lower Tagora consists of the Guezouman medium to coarse sandstones and the Tchinezogue argillites and fine sandstones. The Upper Tagora consists of the Tarat medium to very coarse sandstones, the Madaouela silts and the argillaceous sandstones and lacustrine shales of the Arlit formation;
- A sequence called the "Continental Intercalaire" from Permian to Jurassic, which consists mainly of fluvial sandstone sediments with intercalation of lacustrine argillites;
- The Lower Cretaceous consists of the Irhazer shale formation, with the silts and fine sandstones of the Assaouas at its base.

The main structural feature of the Tim-Mersoi basin is the north-trending In Azawa lineament - Arlit fault, which extends over hundreds of kilometers through the basin to Algeria. The Air massif basement is strongly folded and influenced by two major structures, oriented N20-N30 and N135 degrees. In the Arlit area, the N20-N30 direction predominates and corresponds to the main lineation and structural feature (Figure 4) [20]. The sedimentary cover's deformation results from basement faulting, with several N30 lineaments offset by N80 structures [20]. The N30 flexures are the direct result of the vertical displacement of the Arlit normal fault, active during the sedimentation phase. At the base of the Tarat sandstone, these structures played a major role in forming a major synclinal axis and paleochannels, favorable uranium traps. Geological host formations gently dipped southwestward and lay 150 m deeper west of the Arlit fault. All known economic deposits are located east of the fault [21], and Arlit deposits are hosted in the Upper and Lower Visean Carboniferous formations of the Tarat and Guezouman, rich in organic matter [21-24,31].

2. Materials and Methods

The methodological approach adopted for this work consists of fieldwork and laboratory analysis:

2.1. Fieldwork

The fieldwork in this study involves a detailed cuttings survey of exploration boreholes in Tamari Prospect. These holes were drilled in the Tamari prospect at 100m x 100m and 100 centered and continued until reaching the terminal formation of Thinezogue. The cuttings of exploration drilled boreholes were properly cleaned to remove the drilling mud and range at 10m each. The applied technique for the cuttings survey consists of a macroscopic assessment of oxide-hydroxide indices. In this technique, we first proceed to the general delineation of Izegouande, Arlit, Tarat, and Tchinezogue formations, then follow up with intra-delineation within each formation based on the variations of colors, grain sizes, and oxydo-reduction of the cuttings. Secondly, we described the different indexes of cuttings.

The color of the cutting is attributed by using a chart of color. The granulometry is usually determined on a grain size chart proposing the different sizes of the grains from the clays to the micro conglomerates **(**Figure 5**).** The oxide-hydroxides have resulted mainly from the alteration of ferrous minerals. For the evaluation index of these parameters, we generally use the color of the facies where 0 is related to Black, light gray, green-gray, and green colors, indicating the absence of oxidation; 1 is linked to Yellow-green, yellow, yellow-brown, brown indicate marked oxidation (goethite) while 2 represent Red-brown, red-orange, red, purple, pink related to intense or extreme oxidation (hematite)

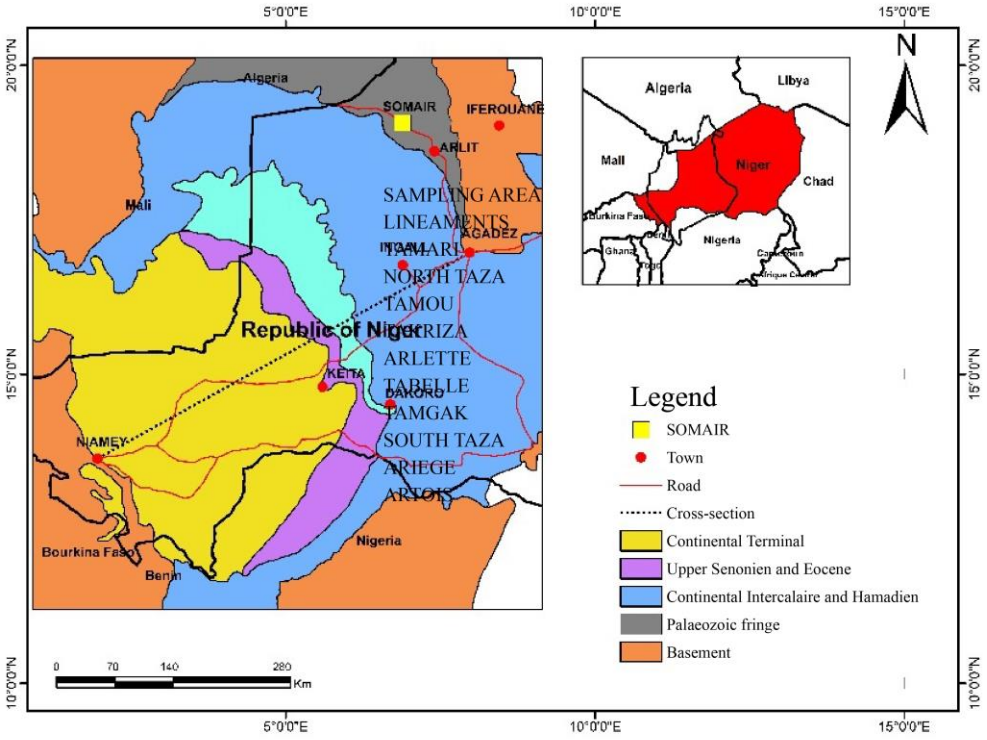

Fig. 2 Niger general geological map

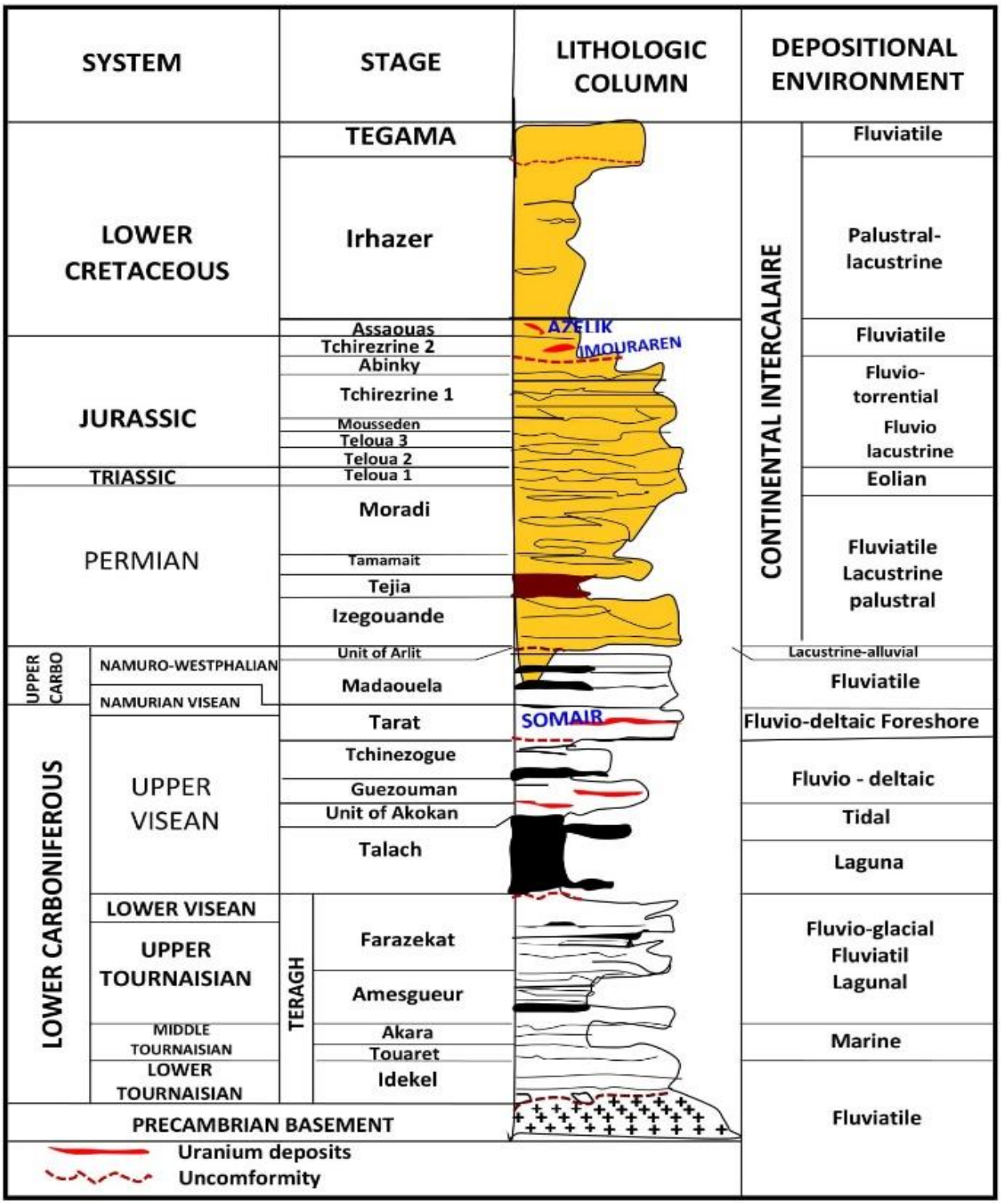

Fig. 3 Litho-stratigraphic Colonne of sedimentary series from Devonian to lower cretaceous with the corresponding depositional environment in Tim-Mersoi basin after [31] modified.

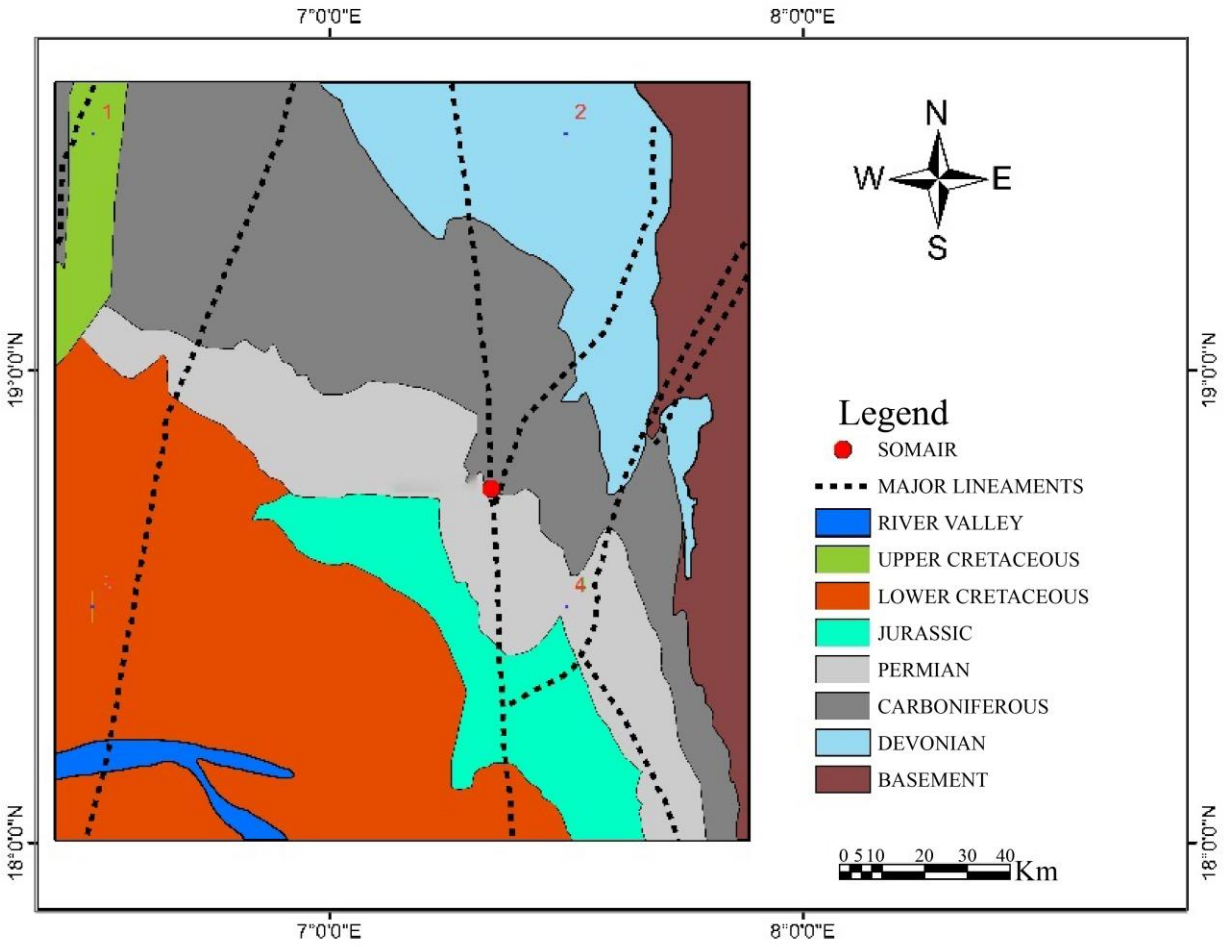

Fig. 4 Geological and structural map of the edge of the Tim-Mersoi basin showing the study area and economic or sub-economic deposits of the Arlit region [31] modified.

3. Results and Discussion

3.1. Delineation of Different Formation

The observation of drilling cuttings allows us to distinguish four formations in the Tamari sector. These four formations consist of Izegouande, Arlit, Tarat, and Tchinezogue **(**Figure 6**).**

Izegouande formation has a depth varied from 0 to 40 or 50m with an average of 45m in the whole Tamari prospect. It consists of red medium to coarse sandstone feldspar, sometimes microconglomeratic, with siliceous cement, sometimes carbonate or kaolins. Several levels of clay are distinguished within this set of high-energy deposits. Their number and thickness are variable. In some areas, Izegouande becomes much more clayey in its upper part and is in the form of an alternation between planimetric sandstone benches and interbank metric clay banks. Based on the logging data, the bottom of Izegouande is marked by a very clear level of resistivity, corresponding to a very coarse level of conglomeratic sandstones.

The Arlit formation is recognized by the sandstone facies rich in aeolian elements (blunted grains) and by greenish clay chips and wine bindings. When Arlit does not have a large proportion of blunted quartz grains, the boundary between the Izegouande base and the alarm wall is quite difficult to determine. It is usually the color change and the disappearance of the feldspars which makes it possible to position the stratigraphic limit.

The Tarat formation is divided into four units (U4, U3, U2, and U1) based on the geophysical results (Beaudoin, 1984). As such, Unit4 (U4) consists of reduced gray fine consolidated sandstone alternating clay-silt; Unit 3 (U3) is composed of coarse to medium sandstone with increasing presence of micro-conglomerate towards the bottom; Unit 2 (U2) is characterized by reduced fine gray sandstone with kaolinitic cement and Unit 1 (U1) consists of coarse to micro-conglomerate gray sandstone **(**Figure 6**)**.

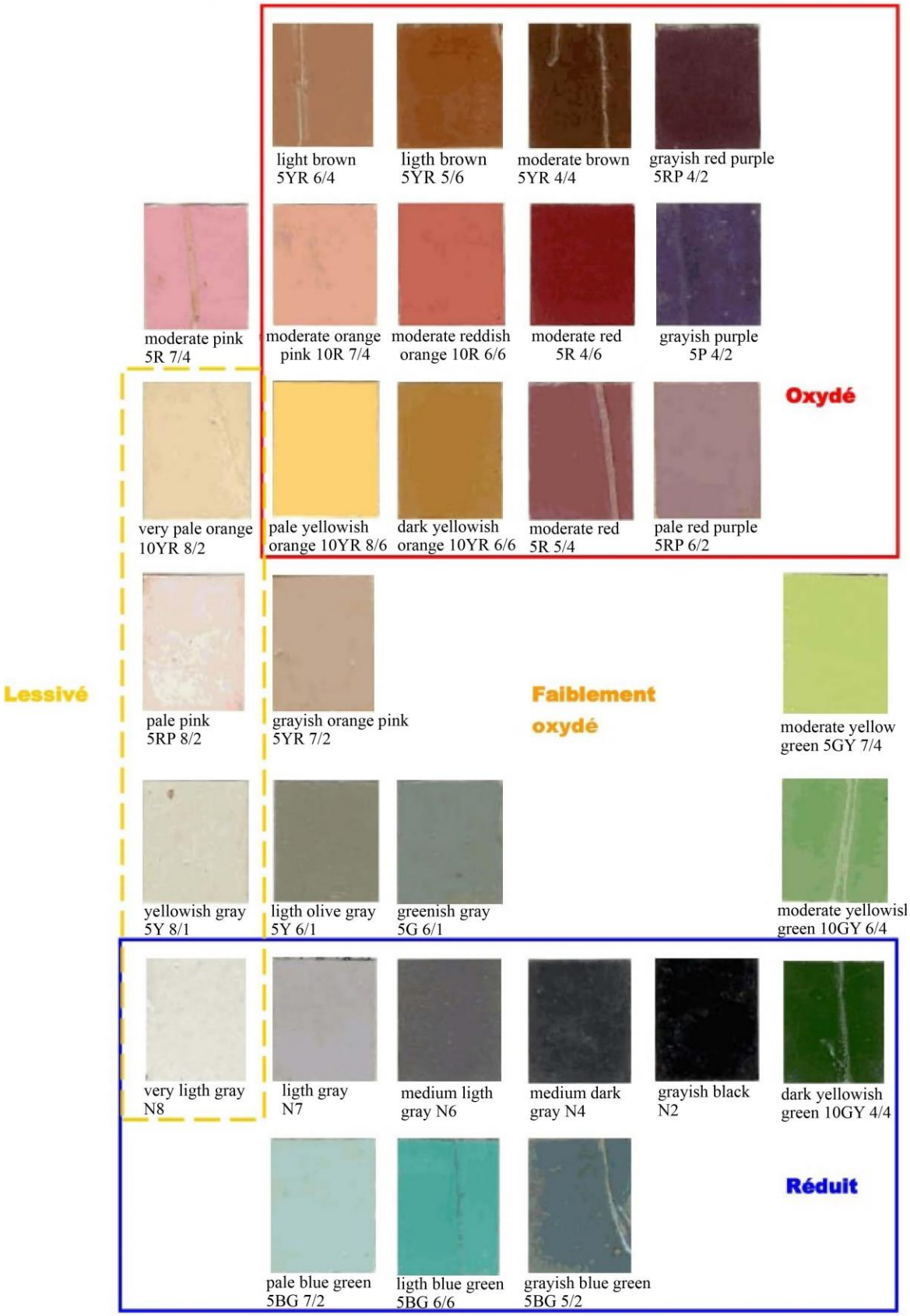

Fig. 5 Color chart standard using in redox mapping

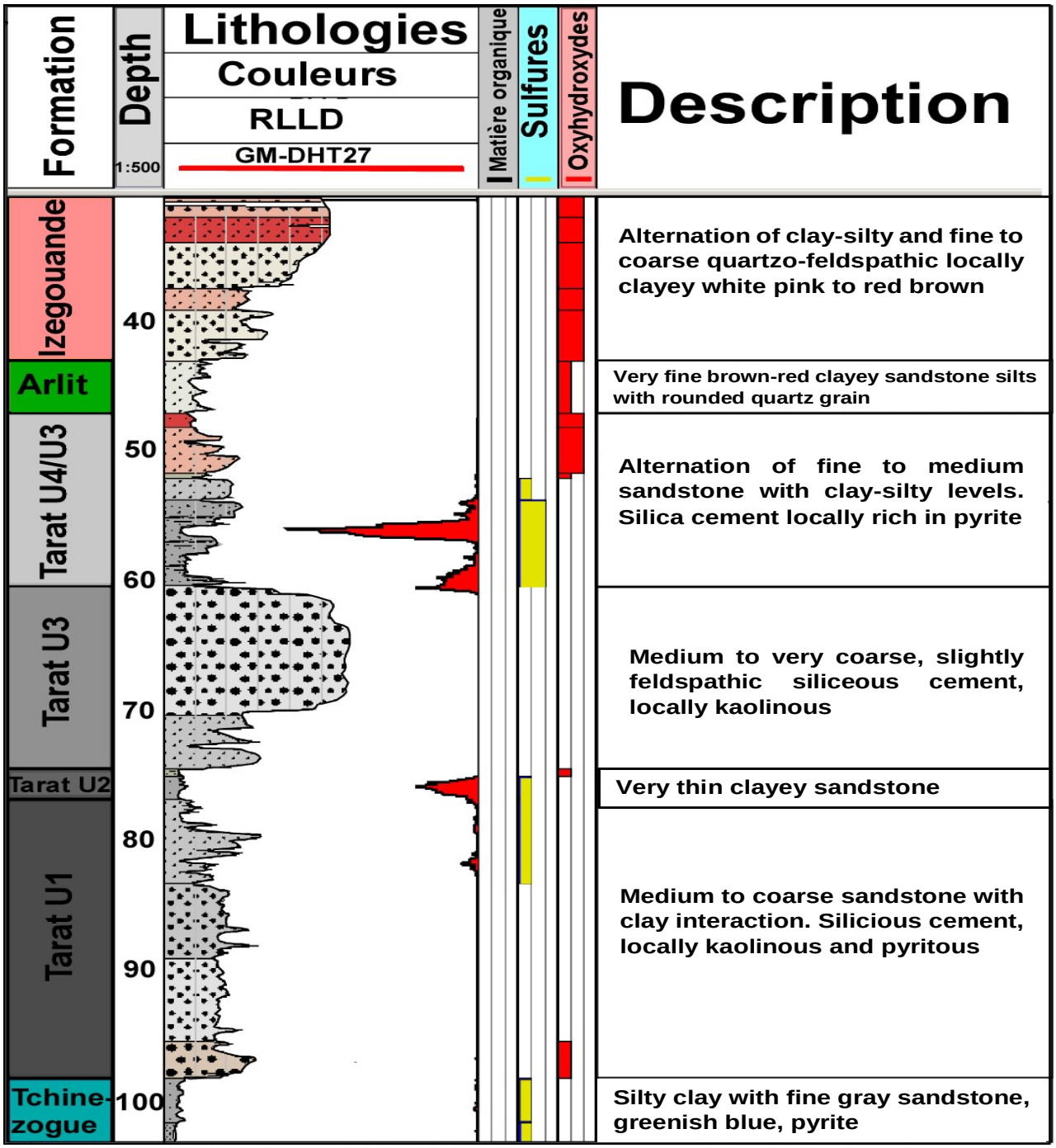

Fig. 6 Lithological logs showing different delineated formations.

3.2. Borehole redox mapping in Tarat formation

The cuttings are recovered every 10 m during the drilling process. The geologist systematically describes cuttings in piles 1, 2, or 3 according to lithological facies, texture, particle size, mineralogy, color, and petrography. This description is made using a magnifying glass that allows seeing well the shape and other characteristics of the grains, the acid pipette, which makes it possible to evaluate the abundance of carbonate, and the color chart. The results of oxide-hydroxide distribution are acquired based on the quantitative assessment of the oxidation state cuttings. All the results are listed in Tables 1 to 4.

Fig. 7 Drill cuttings classified at every 10 m for assessment.

Table 1. Quantitative assessment of the oxidation in the Unit4 (U4)

Drill holes	Depth	Thickness	Oxide-hydroxide
TMRI_0001_1	43.4 - 45.05	1.65	1
TMRI_0001_1	45.05 - 45.56	0.51	0
TMRI_0008_1	42.68 – 43.32	0.64	0
TMRI_0008_2	43.25 – 43.79	0.54	0
TMRI_0011_1	32.22 – 35	2.78	0
TMRI_0012_1	37.98 – 39.98	2	1
TMRI_0013_1	38.89 – 40.4	1.51	0
TMRI_0013_1	40.4 – 41.71	1.31	0
TMRI_0013_1	41.71 – 43.81	2.1	0
TMRI_0015_1	39.91 – 41.08	1.17	1
TMRI_0015_1	41.08 - 42	0.92	0
TMRI_0015_1	42 – 42.87	0.87	0
TMRI_0016_1	42.35 – 43.06	0.71	0
TMRI_0016_1	43.06 – 43.79	0.73	0
TMRI_0017_1	43.61 – 45.18	1.57	0
TMRI_0019_1	45.22 – 46.06	0.84	2
TMRI_0019_1	46.06 – 47.62	1,56	2
TMRI_0019_1	47.62 – 49.02	1,4	1
TMRI_0020_1	51,23 – 51.98	0,75	1
TMRI_0020_1	51.98 – 52.9	0,92	0
TMRI_0021_1	44.68 – 46.51	1,83	2

Table 2. Quantitative assessment of the oxidation in the Unit3 (U3)

Drill holes	Depth	Thickness	Oxide-hydroxide
TMRI_0008_1	60.12 - 61.22	1.1	0
TMRI_0008_2	43.79 - 45.94	2.15	0
TMRI_0008_2	45.94 – 46.95	1.01	0
TMRI_0008_2	46.95 – 48.84	1.89	0
TMRI_0008_2	48.84 – 50.02	1.18	0
TMRI_0008_2	50.02 – 50.57	0.55	0
TMRI_0008_2	50.57 – 50.61	0.04	0
TMRI_0008_2	50.61 – 50.87	0.26	0
TMRI_0008_2	50.87 – 51.31	0.44	0
TMRI_0008_2	51.31 – 51.65	0.34	0
TMRI_0008_2	51.65 – 51.95	0.3	0
TMRI_0008_2	51.95 – 52.2	0.25	0
TMRI_0008_2	52.2 – 52.65	0.45	0
TMRI_0008_2	52.65 – 53.37	0.72	0
TMRI_0008_2	53.37 – 53.7	0.33	0
TMRI_0008_2	53.7 – 54.47	0.77	0
TMRI_0008_2	54.47 – 54.65	0.18	0
TMRI_0008_2	54.65 – 55.2	0.55	0
TMRI_0008_2	55.2 – 55.85	0.65	0
TMRI_0008_2	55.85 – 56.2	0.35	0
TMRI_0008_2	56.2 – 56.95	0.75	0

Table 3. Quantitative assessment of the oxidation in the Unit2 (U2)

Drill holes	Depth	Thickness	Oxide-hydroxide
TMRI_0249_1	59.56 – 64.38	4,82	0,00
TMRI_0250_1	79.90 – 84.74	4,84	0,00
TMRI_0251_1	62.17 -64.00	1,83	0,00
TMRI_0251_1	64.00 – 66.23	2,23	0,00
TMRI_0252_1	64.33 – 67.22	2,89	2,00
TMRI_0253_1	81.49 – 84.74	3,25	0,00
TMRI_0254_1	102.60 – 104.26	1,66	2,00
TMRI_0254_1	104.26 - 107.14	2,88	0,00
TMRI_0255_1	91.65 – 93.04	1,39	0,00
TMRI_0256_1	94.83 – 99.63	4,80	0,00
TMRI_0257_1	86.65 – 87.77	1,12	0,00
TMRI_0258_1	79.11 – 81.52	2,41	0,00
TMRI_0259_1	64.54 – 67.56	3,02	0,00
TMRI_0259_1	67.56 – 68.80	1,24	0,00
TMRI_0259_2	64.71 - 68.13	3,42	0,00
TMRI_0259_2	68.13 – 69.50	1,37	0,00
TMRI_0259_2	69.50 – 69.96	0,46	0,00
TMRI_0260_1	64.98 – 67.96	2,98	0,00
TMRI_0261_1	65.14 – 67.92	2,78	0,00
TMRI_0262_1	63.85 – 65.65	1,80	0,00

Table 4. Quantitative assessment of the oxidation in Unit1 (U1)

Drill holes	Depth	Thickness	Oxide-hydroxide
TAMR_01_1	80.75 – 86.59	5.84	0
TAMR_01_1	86.59 – 90.4	3.81	0
TAMR_01_1	90.4 – 91.55	1.15	1
TAMR_01_1	91.55 – 93.36	1.81	0
TAMR_02_1	97.09 – 98.81	1.72	0
TAMR_02_1	98.81 – 99.4	0.59	0
TAMR_02_1	99.4 – 101.9	2.5	0
TAMR_02_1	101.9 – 103.94	2.04	0
TAMR_02_1	103.94 – 104.6	0.66	0
TAMR_02_1	104.6 – 108.6	4	0
TAMR_04_1	82.65 – 90.98	8.33	1
TAMR_04_1	90.98 – 93.55	2.57	0
TAMR_04_1	93.55 – 97.93	3.93	1
TAMR_04_1	97.48 – 99.75	2.27	0
TAMR_04_1	99.75 – 100.98	1.23	1
TAMR_04_1	100.98 – 102.59	1.61	1
TAMR_04_1	102.59 – 103.76	1.17	0
TAMR_05_1	100.13 – 102.08	1.95	0
TAMR_06_1	75.81 – 76.9	1.09	0
TAMR_06_1	76.9 – 80.18	3.28	0

3.2.1. Redox in Tarat Unit4

The Trarat unit4 or Tarat-Madaouella is found at a depth of 50 to 75 m with an average of 63 m. It has a small overall thickness variation of 1 to 12m (Figures 8 and 9). In the plateau context, the predominance of the sandstone or alternating Madaouda characteristics is due to variations in facies and low thicknesses.

The distribution maps of oxyhydroxides in the Tarat Unit4 (U4) show intense oxidation traces scattered throughout the investigated prospect (Figure 10); almost 80% of the indices are between 1.01 and 3.00, while the distribution maps of oxyhydroxides and mineralization of this unit show that the strong radiometric accumulations (2.01 to 10.00 ‰) are mainly concentrated in the zones of low accumulation in oxyhydroxides (0.26 to 0.70) (Figure 11).

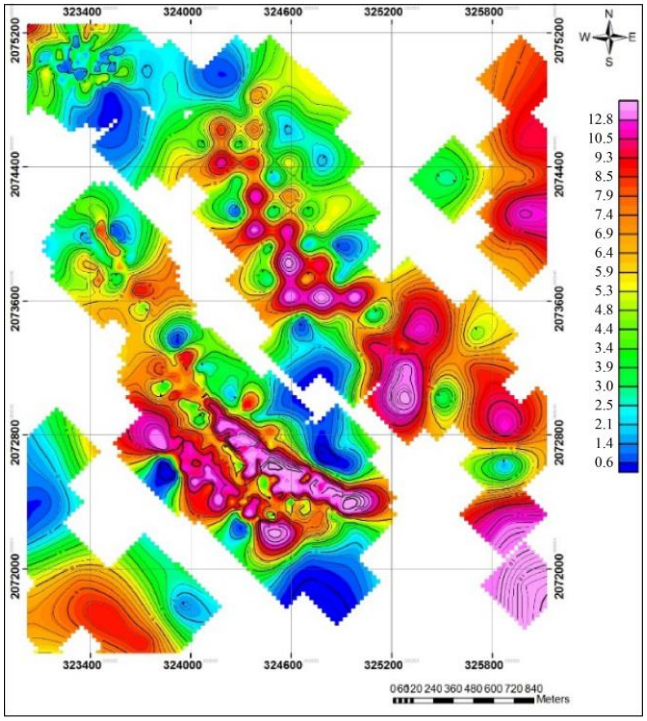

Fig. 8 Isopach map of Tarat Unit4

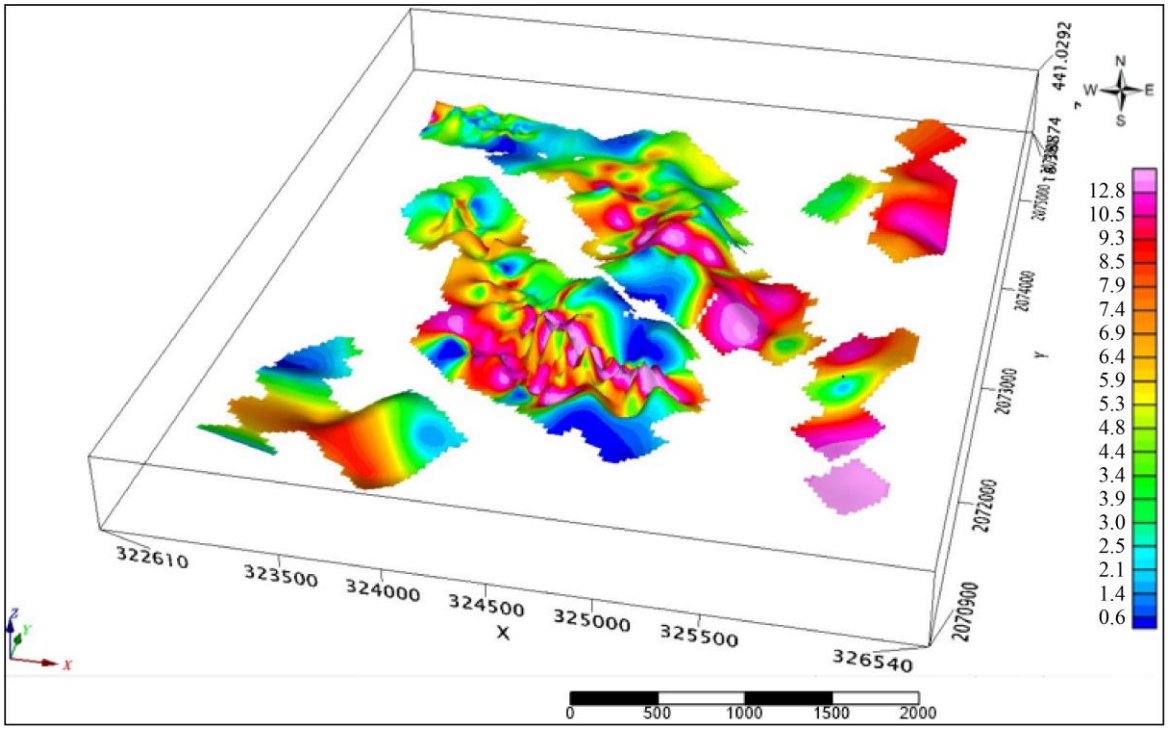

Fig. 9 3D isopach map of Tarat unit4.

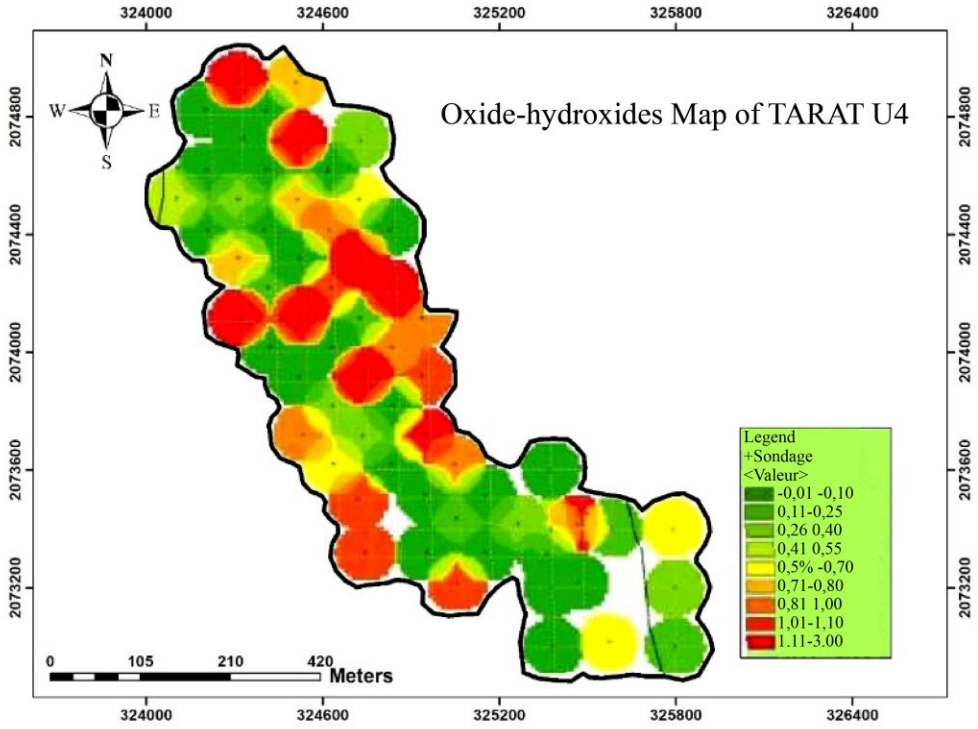

Fig. 10 Oxide-hydroxides distribution map in the Tarat Unit4 (U4).

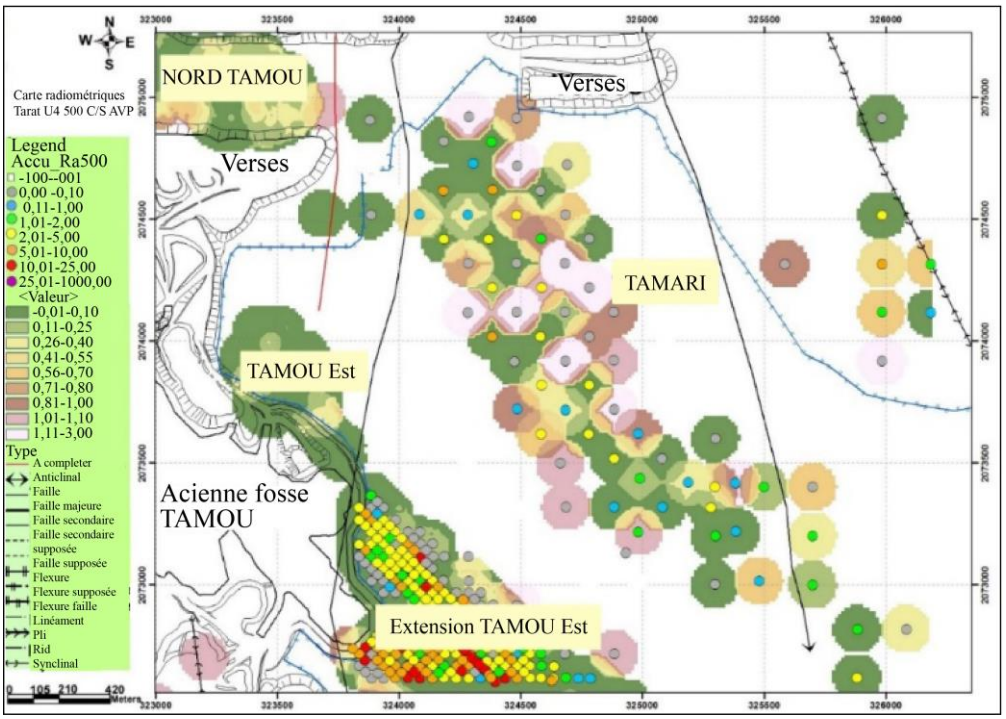

Fig. 11 Map of distribution of oxyhydroxides associated with radiometry in Tarat Unit4 (U4)

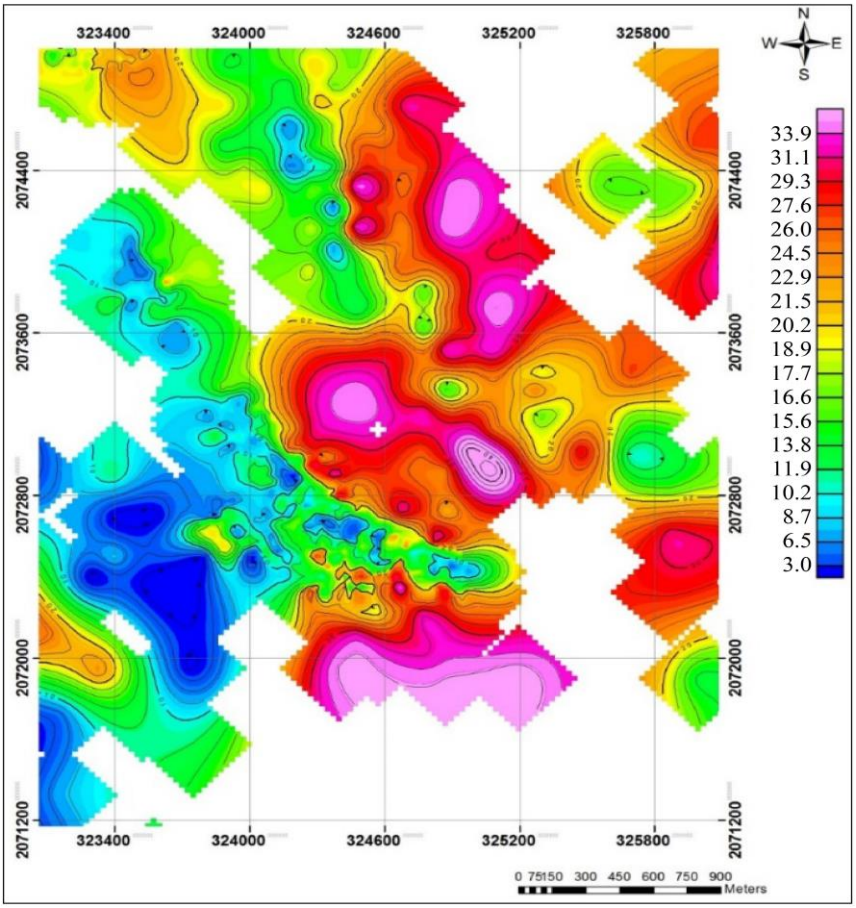

Fig. 12 Isopach of Tarat Unit3

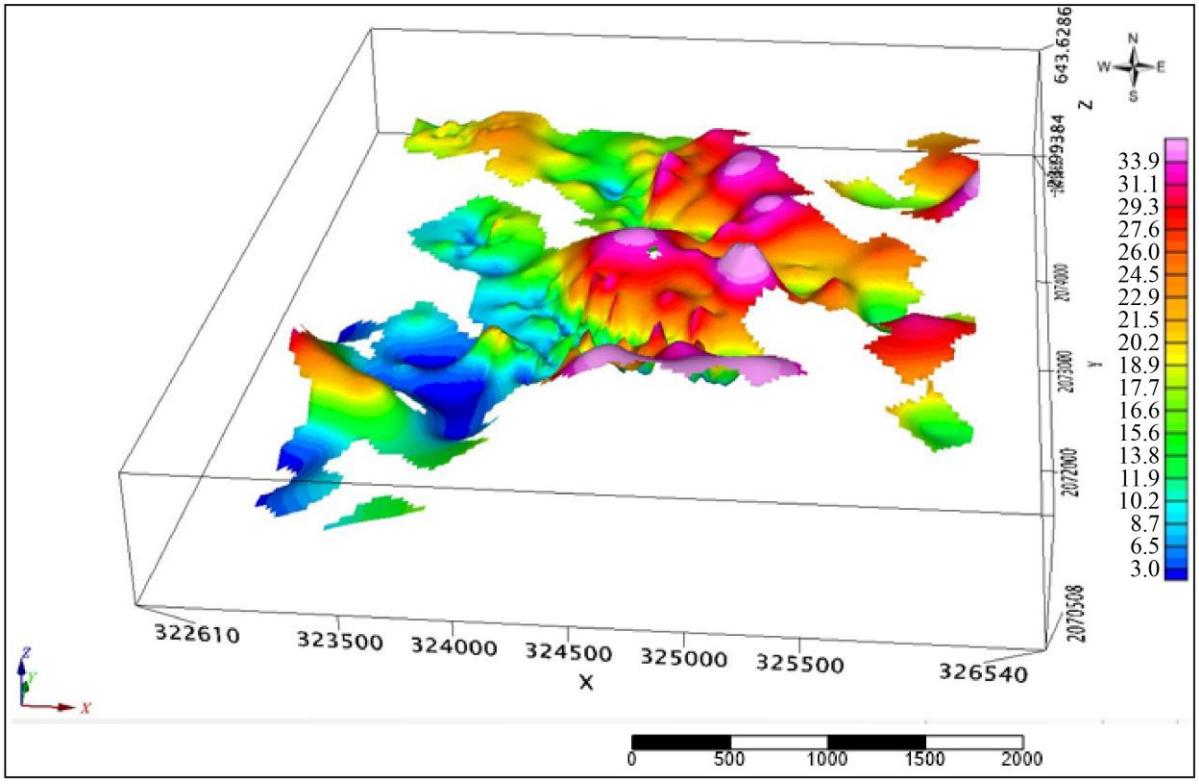

Fig. 13 3D isopach map of Tarat Unit3.

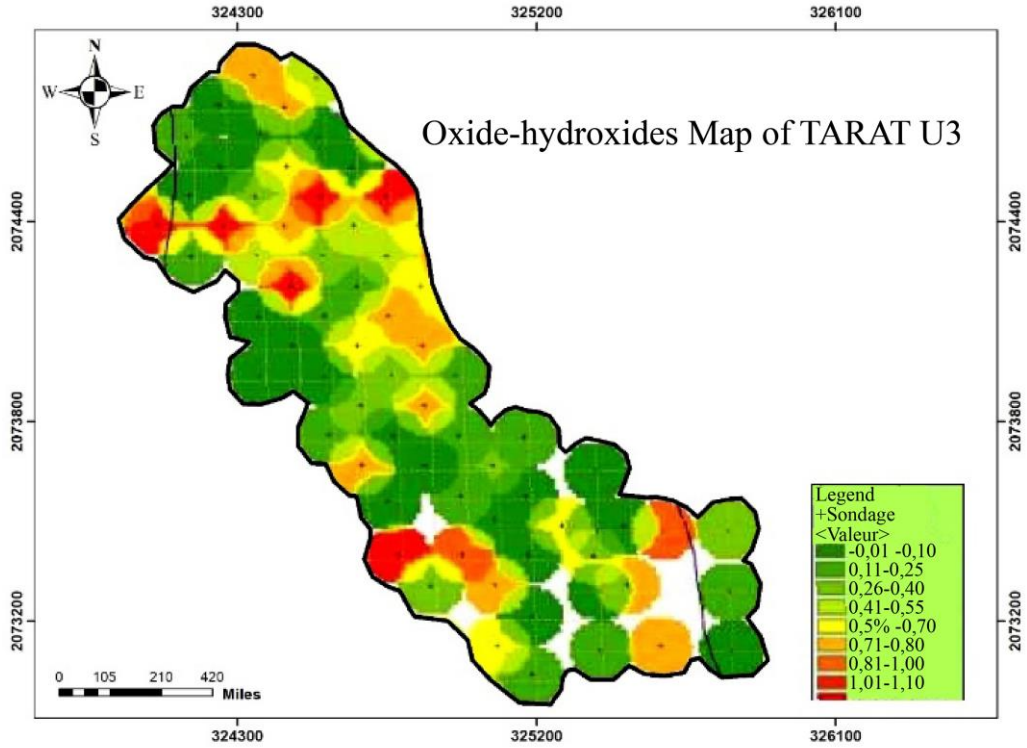

Fig. 14 Oxide-hydroxides distribution map of Tarat Unit3 (U3).

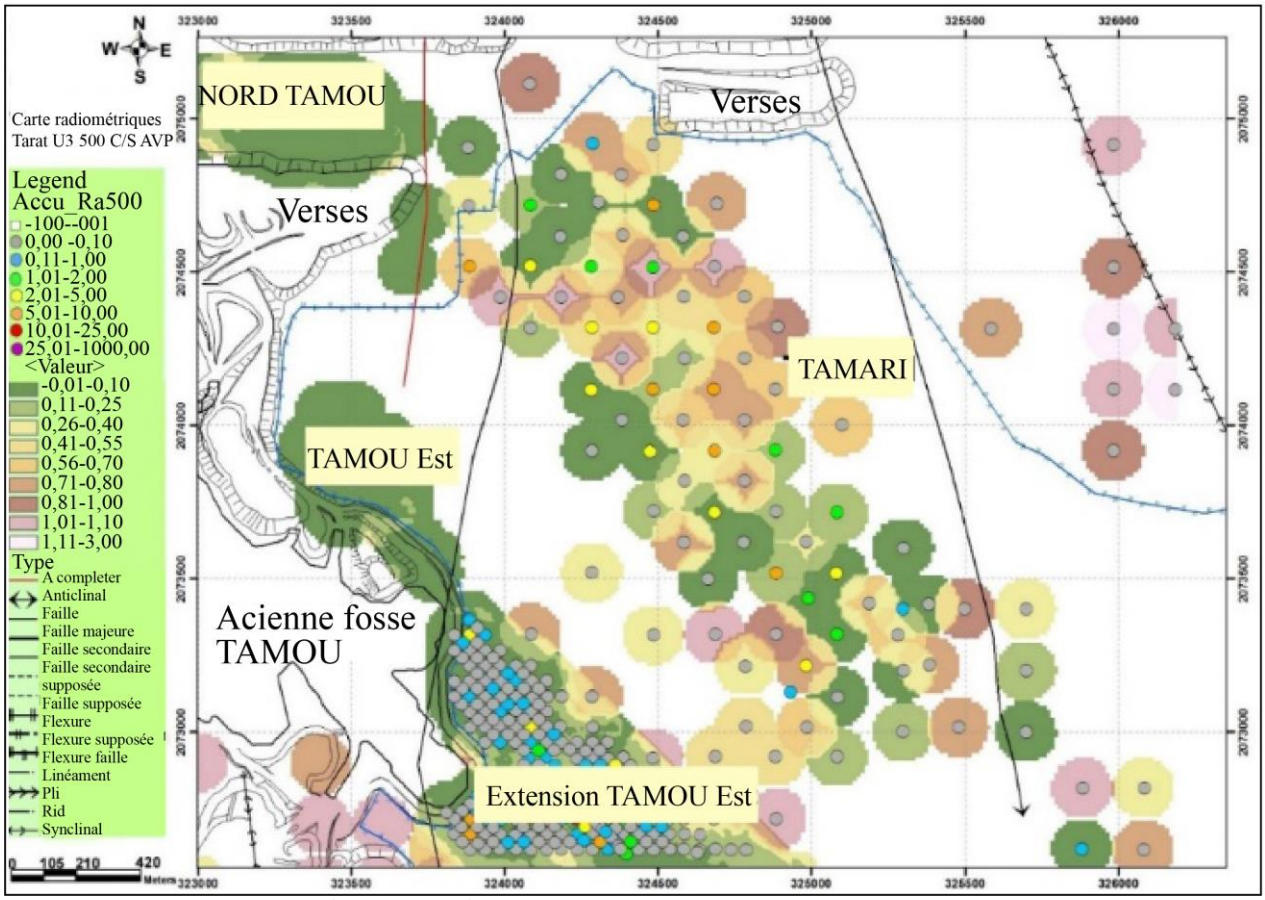

Fig. 15 Map of distribution of oxyhydroxides associated with radiometry in Tarat Unit3 (Unit3)

3.2.2. Redox in Tarat Unit3

The Tarat Unit3 (U3) is represented by alternations of medium to coarse sandstone with siliceous cement, blackish clay, often kaolin, and clay silts. This unit is rich in organic matter and pyrite. The facies are relatively heterogeneous (frequent intercalations of clays). At the bottom, this unit consists of coarse to very coarse sandstones (called coarse U3 Tarat). It is usually oxidized. Reduced clay levels of low thickness (<1m) are locally identified. These coarse to very coarse sandstones are generally well contrasted with the overlying sandstone / clay-silt overlying portion and the underlying sandstone-silty facies unit.

The analysis of the isopach map (Figures 12 and 13) shows that this unit has large variations in thickness at NNE and E, ranging from 20 to 40 m approximately. The smallest thicknesses are located in the South-West and the North, which goes from 3 to 20 m. In general, this Unit3 (U3) seems to be the most oxidized part of Tarat, with almost 50% of indices between 0.56 and 1.00 and located in the northeastern and southern parts of the area (Figure 14). Therefore, the distribution maps of oxyhydroxides and mineralization of this unit show that the strong radiometric accumulations (2.01 to 10.00 ‰) are mainly concentrated in the zones of low accumulation in oxyhydroxides (0.26 to 0.70) (Figure 15).

3.2.3. Redox in Tarat Unit2

The Tarat Unit2 is defined by argillite/fine-grained alternations with siliceous, kaolins, and blackish clayey cement whose thickness varies from 2 to 10m (Figures 16 and 17). The U2 has small variations overall; this unit's large thicknesses of 5.5 to 9 m are also located in the eastern part and a little to the South. U2 is reduced and rich in organic matter and pyrite.

The Unit2 (U2) of the Tarat is reduced as a whole but shows traces of oxidation in the South of the prospect (Figure 18) and some marks in the North. The indices are between 0.56 and 3.00.

The distribution maps of oxyhydroxides and radiometry of Tarat U2 show that this unit is mineralized essentially in the reduced zones near the oxidized zones. Tarat U2 is the smallest unit in the sector, with few oxidized zones. The accumulations have a content between 0.11 and 5 ‰ and a direction N-S (Figure 19).

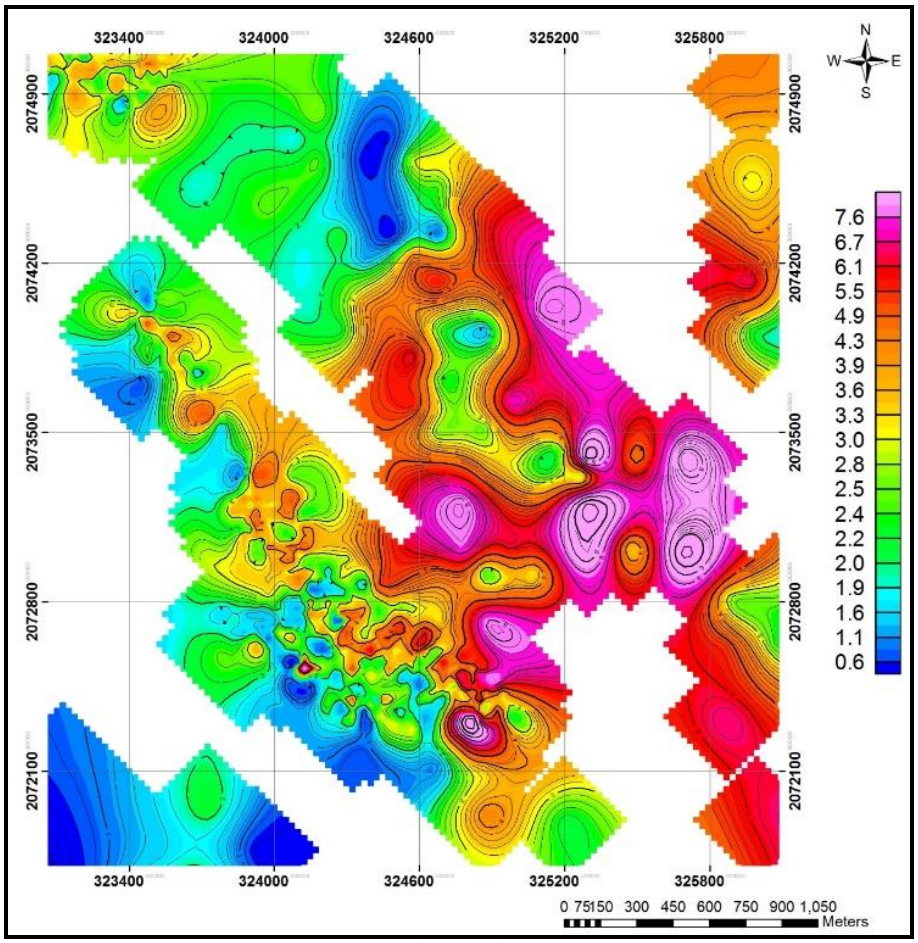

Fig. 16 Isopaque of unit 2 of Tarat (Tarat U2).

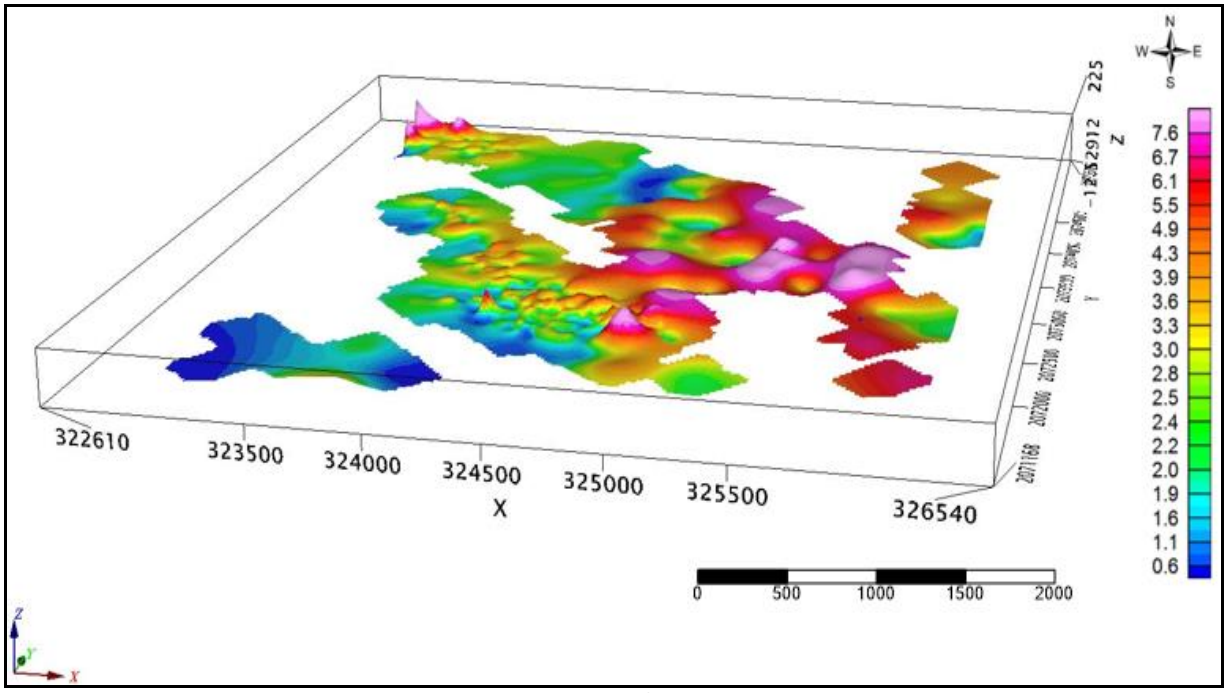

Fig. 17 3D isopach map of Tarat Unit2 (U2).

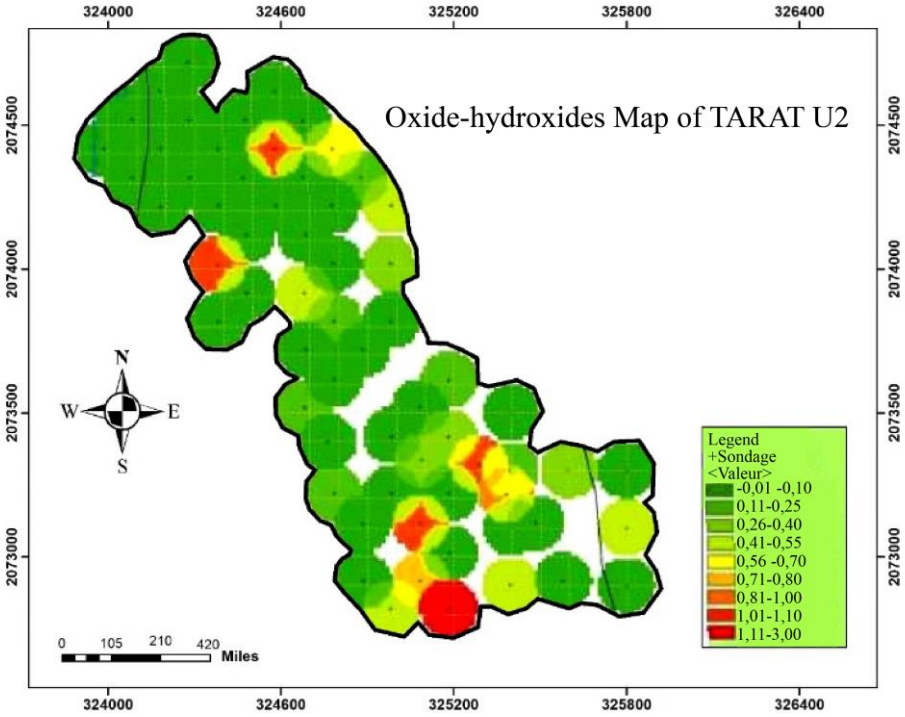

Fig. 18 Oxide-hydroxides distribution map in the Tarat Unit2 (U2).

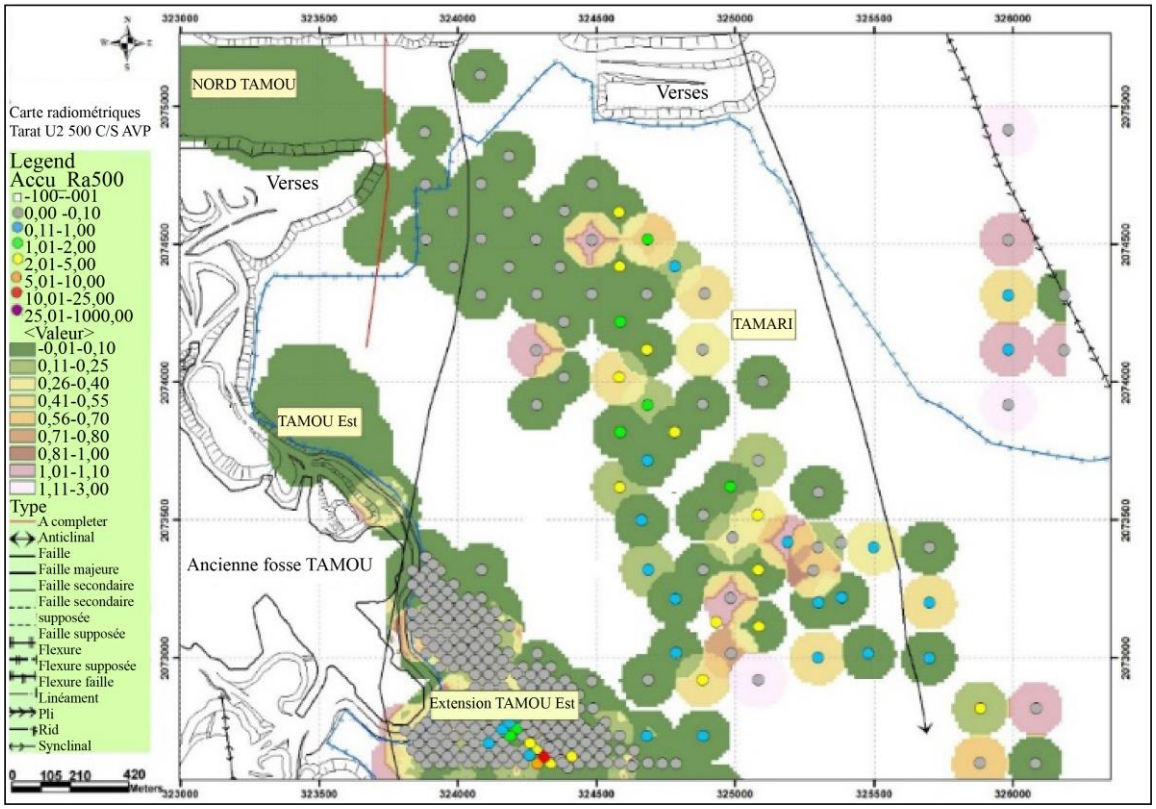

Fig. 19 Distribution map of oxyhydroxides and radiometrics in Unit 2

3.2.4. Redox in Tarat Unit1

The Tarat Unit1 is a coarse to medium sandstone sequence with siliceous cement, locally kaolins, well consolidated with abundant organic matter and pyrite. The isopach maps of Unit 1 show thicknesses ranging from 5 to 25 m. The large thicknesses of 20 to 25m are located in the East and the South, and the small thicknesses of 5 to 15 m are in the North-West and North-East (Figures 20 and 21).

The oxide-hydroxides of Tarat Unit1 are generally located northeast and South of the Tamari prospect, and most of the accumulations are between 0.58 and 0.8. The strong indices located at the extreme northeast are between 1.1 and 3.00 (Figure 22). The distribution maps of oxyhydroxides and radiometry of Tarat U1 show that this unit is mineralized essentially in the reduced zones near the oxidized zones with an accumulations content between 0.11 and 5 ‰ (Figure 23)

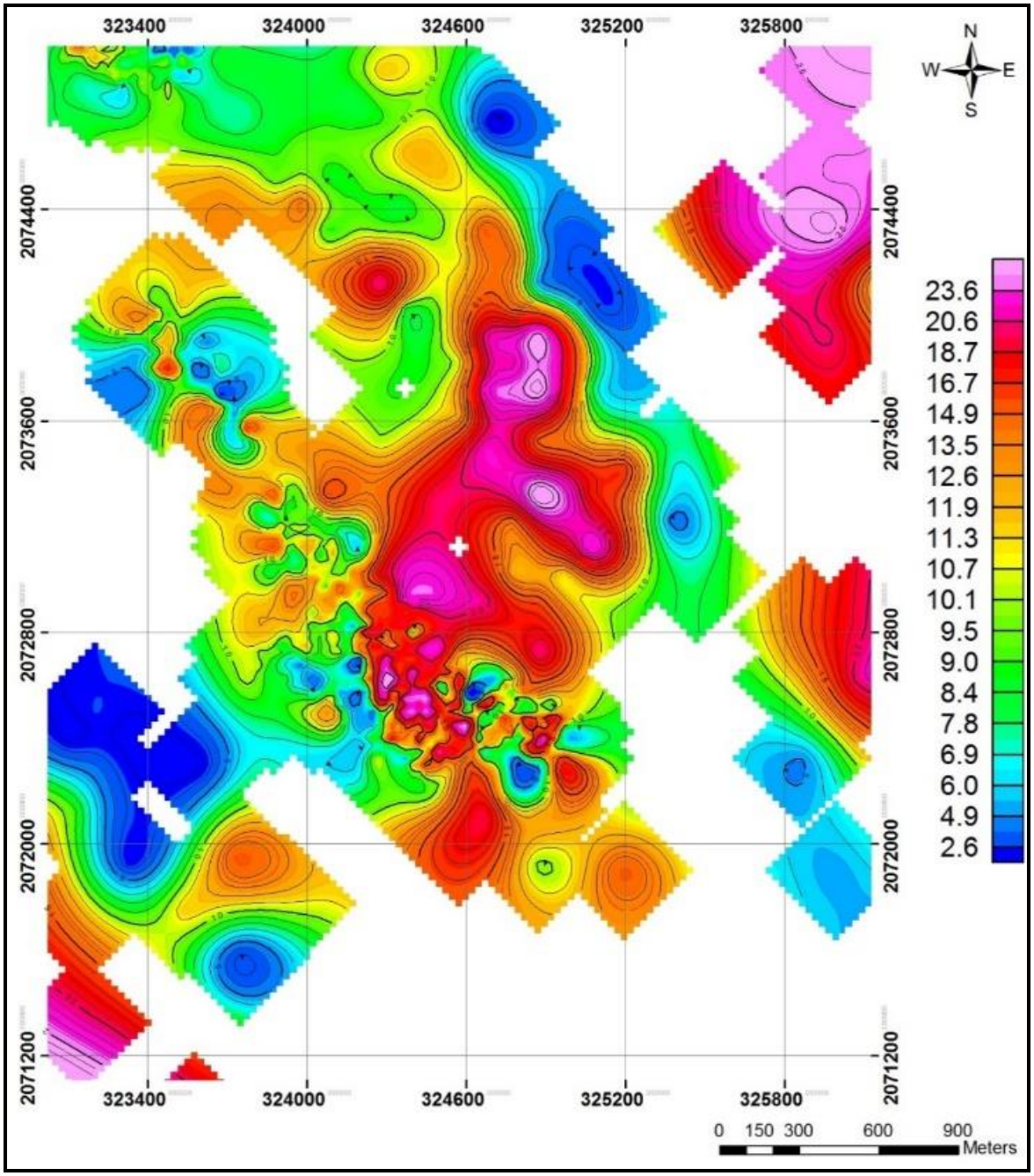

Fig. 20 Isopach map of Tarat Unit1

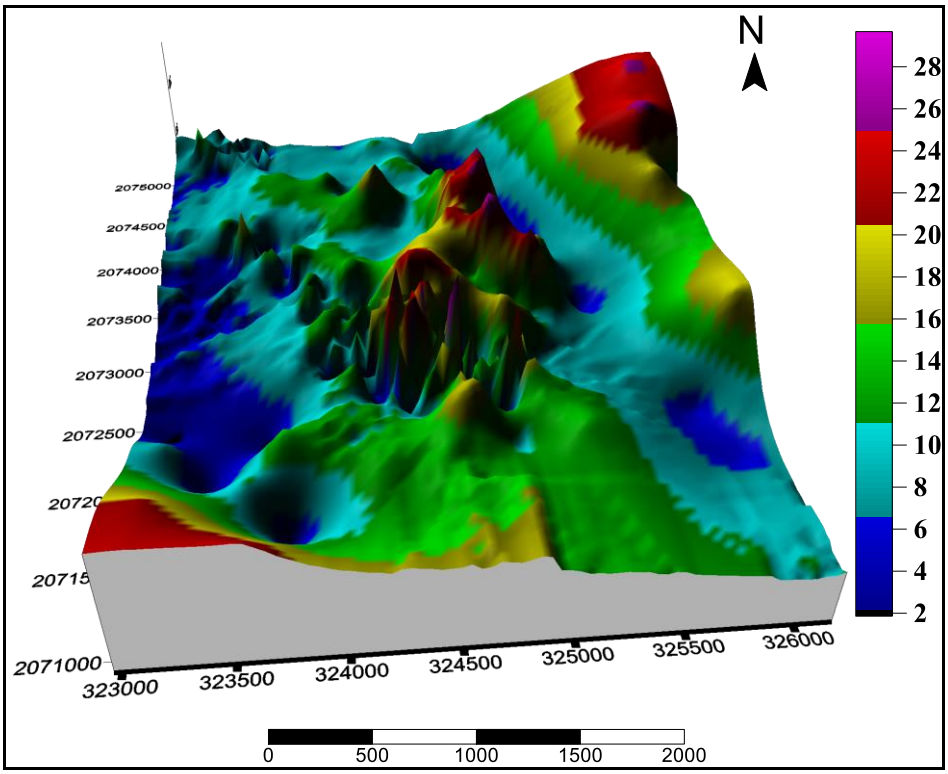

Fig. 21 3D isopach map of Tarat Unint1 (U1)

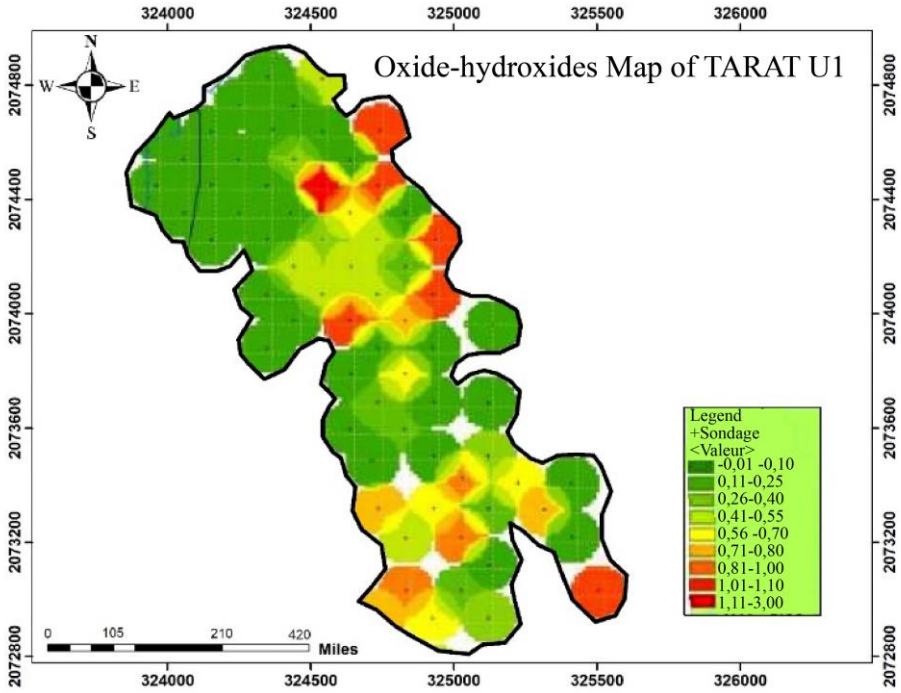

Fig. 22 Oxide-hydroxides distribution map of Tarat Unit1 (U1).

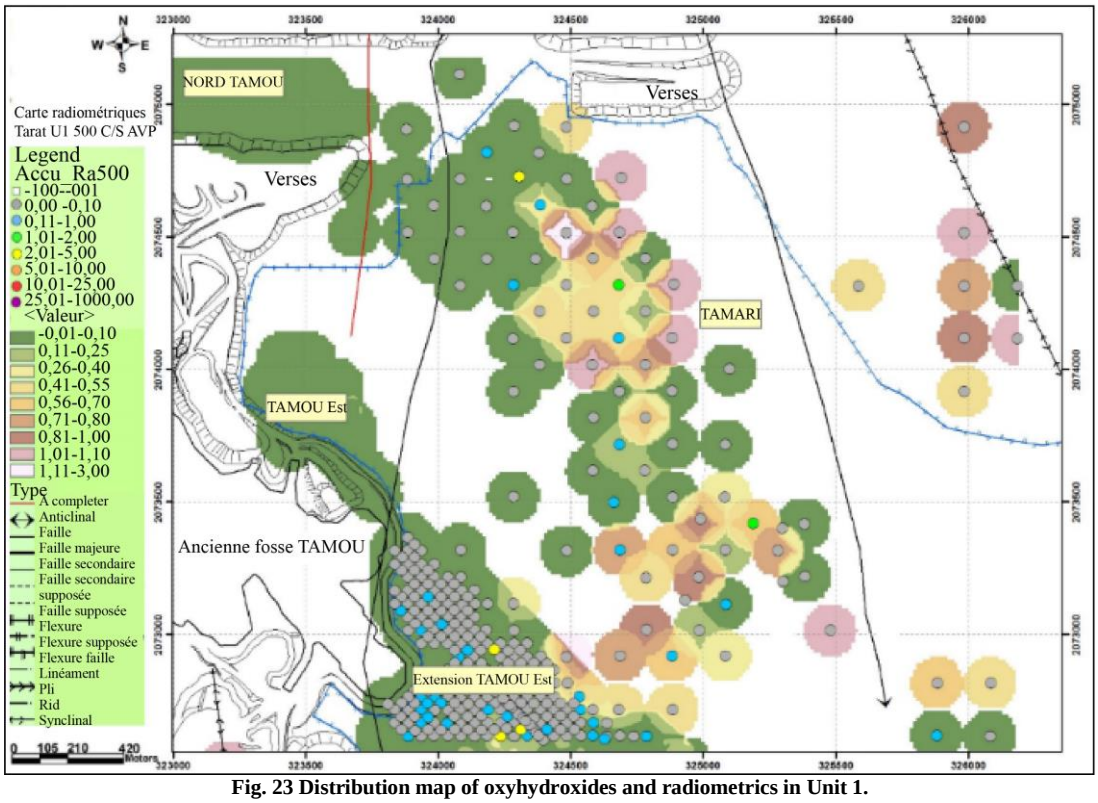

Fig. 23 Distribution map of oxyhydroxides and radiometrics in Unit 1.

3.3. Interpretation of redox and mineralization in the whole Tarat

The map below in figure 24 provides an overview of the 2016 Tamari radiometric survey results (total accumulations). The stratigraphic correlation base radiometric response in the boreholes TMRI 0113, TMRI 0420, TMRI 0116, TMRI 0001, TMRI 0382, TMRI 0107, and TMRI 0021indicates that units U3, U2, and U1 are poorly mineralized. At the same time, major ore bodies occur along the lateral and terminal edges of the Unit (U4). The majority of the U-mineralization in these deposits occurs within the sandstone. However, a minor amount of U also exists within mudstone and siltstone, where U is generally intermixed with carbonaceous debris and mainly occurs as unidentified, fine-grained [26-28] (Figure 25).

The isopach map (Figure 26) shows two main variations in thickness; a variation of 50 to 60 m in the North-East and South parts and a variation of 20 to 50 m in the South-West part, North-West. The 3D model of the Isopaque map of Tarat (Figure 27**)** shows that this formation has zoned in the form of gutters favorable to the accumulation of organic matter and pyrite. The Tarat formation in the study area is oxidized mainly in the northeast and South of the prospect, but areas with moderate oxidation were favorable for the deposition of mineralization. These zones located mainly at the interface oxidized and reduced zones correspond to redox fronts.

The distribution maps of oxyhydroxides and mineralization of Tarat-Madaouela and Tarat U3 show the strong radiometric accumulations (2.01 to 10.00 ‰) are mainly concentrated in zones of low accumulation in oxyhydroxides (0.26 to 0.70). The latter probably corresponds to redox fronts (interface between the reduced zones and the oxidized zones). The redox fronts are suitable environments for trapping uranium [26-29]. The contact between a mineralized oxidizing medium and a reduced medium favors the trapping of U by the M.O and sulfides [29]. These units are moderately to slightly oxidized overall. The circulation of fluids favors this oxidation. We also note that the mineralization has North-West-South-East (N130) direction.

The distribution maps of oxyhydroxides and radiometry of Tarat U2 and Tarat U1 show that these units are mineralized essentially in the reduced zones near the oxidized zones. Tarat U2 is the smallest unit in the sector, with few oxidized zones. The accumulations have content between 0.11 and 5 ‰ and N-S (in Unit 2) direction.

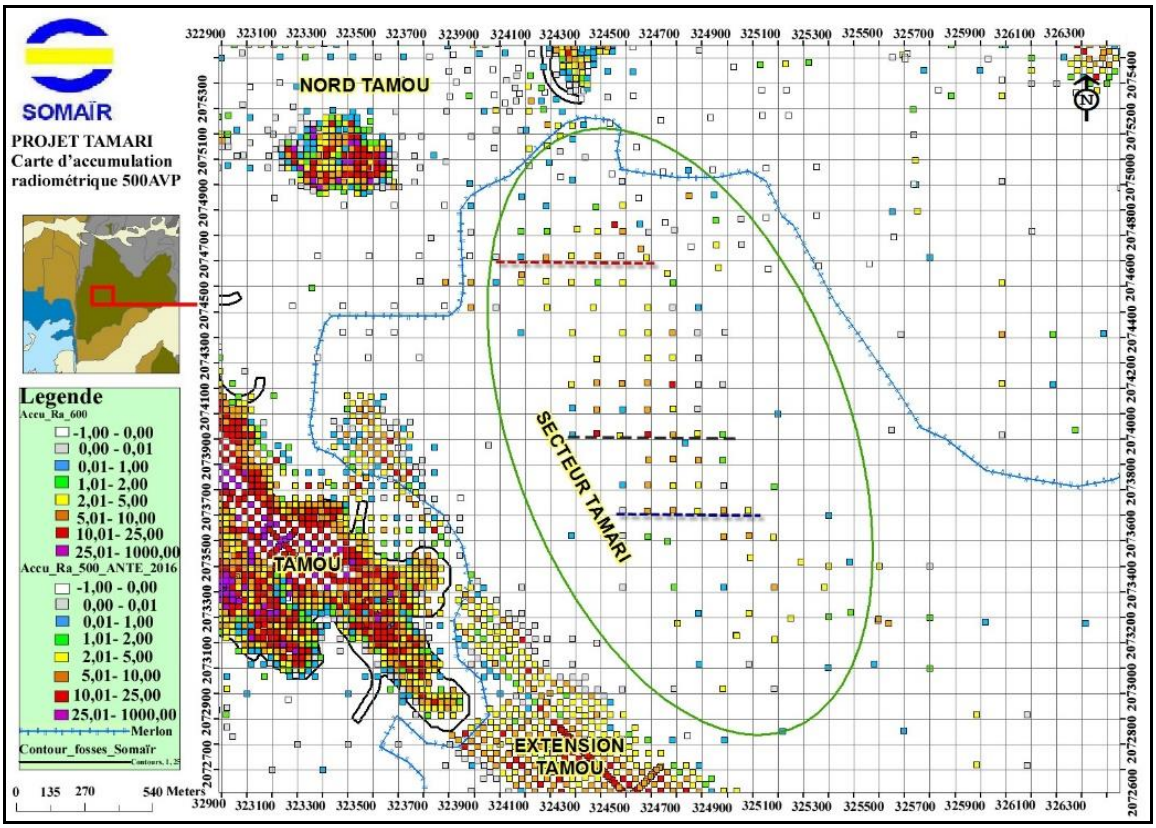

Fig. 24 Radiometric map of the Tamari sector

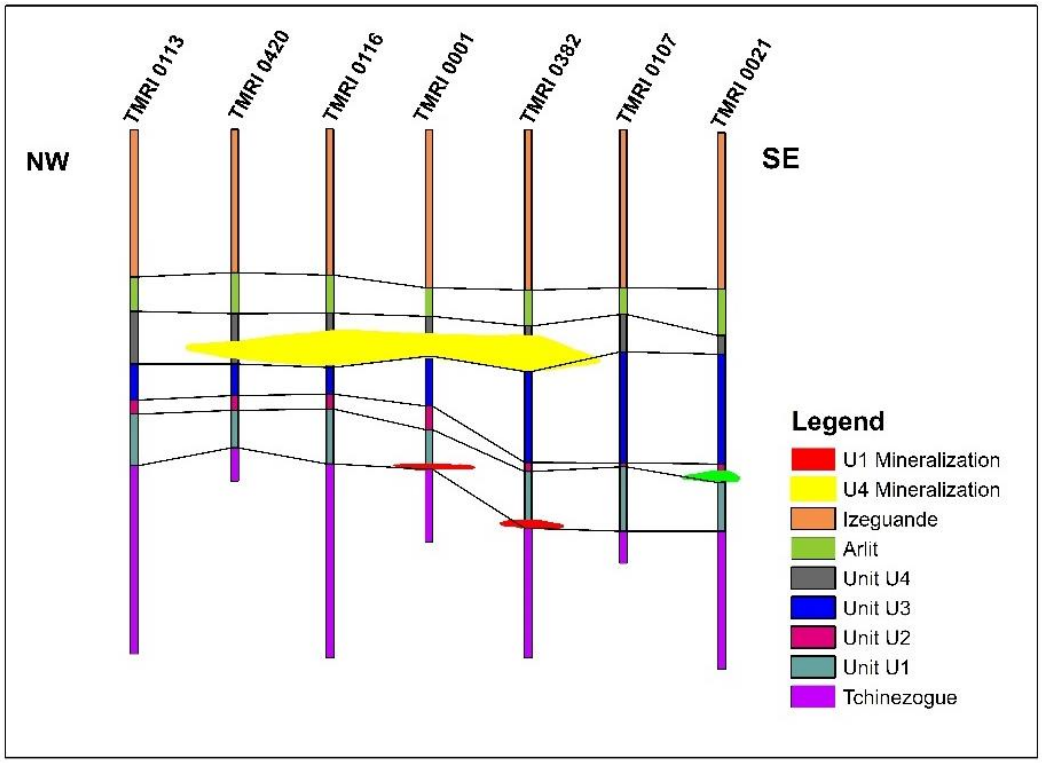

Fig. 25 Stratigraphic correlation delineated uranium mineralization in the whole Tarat formation.

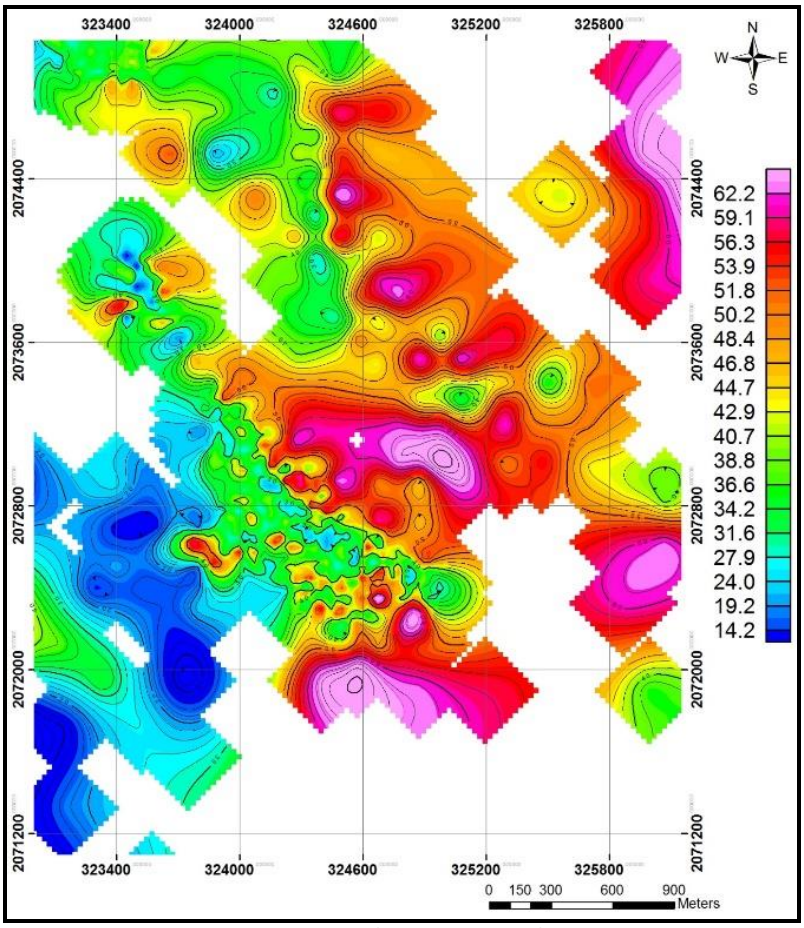

Fig. 26 Isopach map of the whole Tarat formation.

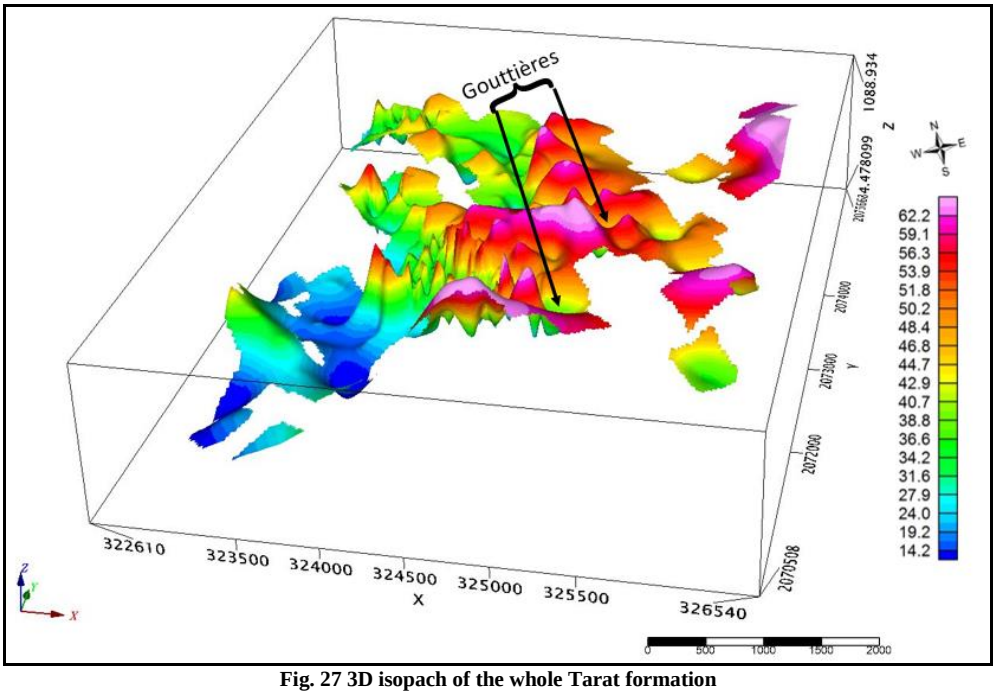

Fig. 27 3D isopach of the whole Tarat formation

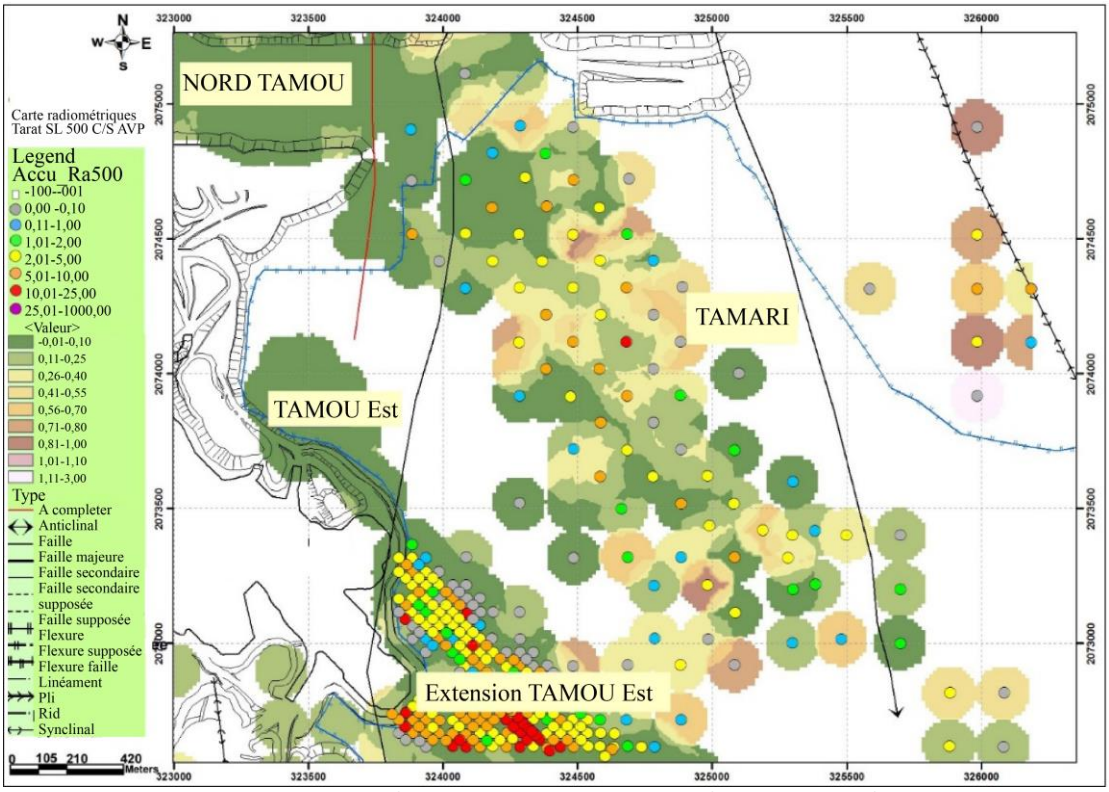

Fig. 28 Distribution map of oxyhydroxides and radiometric of the whole Tarat formation

4. Conclusion

The Tarat formation in the Tamari prospect was deposited in a fluvial-deltaic environment rich in organic matter. Circulations of oxidizing fluids after the deposition have partially oxidized the formation creating oxidation-reduction fronts at the oxidized zones-reduced zones interface. Accumulation maps of oxyhydroxides show the existence of a well-defined distribution of the redox parameter.

Oxyhydroxides characterize the oxidizing environment formed during the circulation of oxidizing fluids which are also mineralizers. Tarat-Madaouela (U4) and Tarat U1 are the richest in organic matter and pyrite. Tarat U3 is the most oxidized due to its particle size favorable to an underground circulation (high porosity).

The distribution radiometric and oxyhydroxide maps show that not all oxidized zones have been favorable for uranium deposits. The highly intense oxidation zone is poorly mineralized. High uranium mineralization is observed in environments with low to very low oxidation. Areas with moderate oxidation were suitable for the deposition of mineralization. These zones located mainly at the interface facies oxidized and reduced facies correspond to redox fronts.

Acknowledgments

The authors are grateful to and acknowledge the efforts of the staff of the geological department of SOMAIR (Arlit) for their collaboration during our fieldwork and for providing data. The corresponding author is grateful to both ministries of mine, Niger and Areva, for administrative assistance in conducting this study—sincere thanks to the reviewers for their observations which have greatly improved the manuscript.

References

[1] R.A. Crawley, H.K Holen, and W.L. Chenoweth, “Geology and application of geologic concepts, Morrison formation, grants uranium region, New Mexico, USA.” *International Atomic Energy Agency*, vol. 408, pp. 199–214, 1985. [Google Scholar] [Publisher Link]

[2] La Somair et al., “Les Mines D’arlit Et D’akokan Et Areva, 2007. [Publisher Link]

[3] Peter Volberding, and Jason Warner, “The Uniqueness of Uranium : The Problematics of Statecraft in Niger,” *The Extractive Industries and Society*, vol. 5, no. 3, pp. 294–301, 2018. [CrossRef] [Google Scholar] [Publisher Link]

[4] Dicarra A., Synthesis of Uranium Exploration Work in the Tim Mersoï Basin (Republic of Niger), COGEMA Niger Report (ref: CN/2005/R/11/AD), p. 213, 2005.

[5] Kache, M, Actual Uranium Mining and Exploration in Niger (IAEA-CN--216), International Atomic Energy Agency (IAEA), p. 1-230, 2014. [Google Scholar]

[6] S.Sindhu et al., "Estimation of Activity Concentration of Uranium and Thorium Using Gross Alpha and Gross Beta in Agricultural Soils in Kanyakumari District," *SSRG International Journal of Agriculture & Environmental Science*, vol. 4, no. 2, pp. 28-35, 2017. [CrossRef] [Publisher Link]

[7] Scholtz. N, Technical Report Batalene 1 and 2 Uranium Projects, Niger, pp. 16-23, 2009.

[8] Milos Rene, "Alteration of Granitoids and Crystalline Rocks and Uranium Mineralization in the Pluton Area, Bohemian Massif, Czech Republic," *Ore Geology Reviews*, vol. 81, pp. 188–200, 2017. [CrossRef] [Google Scholar] [Publisher Link]

[9] Feifei Wang et al., "Relationship between Sandstone-Type Uranium Deposits and Hydrocarbon in the Northern Ordos Basin," *IOP Conference Series: Earth and Environmental Science*, vol. 64, 2017. [CrossRef] [Google Scholar] [Publisher Link]

[10] Ng Ronald, et al., "Oxidation State of Iron in Alteration Minerals Associated with Sandstone-Hosted Unconformity-Related Uranium Deposits and Apparently Barren Alteration Systems in the Athabasca Basin, Canada: Implications for Exploration," *Journal of Geochemical Exploration*, vol. 130, pp. 22–43, 2013. [CrossRef] [Google Scholar] [Publisher Link]

[11] Chunfang Cai et al., "Mineralogical and Geochemical Evidence for Coupled Bacterial Uranium Mineralization and Hydrocarbon Oxidation in the Shashagetai Deposit, NW China," *Chemical Geology*, vol. 236, no. 1-2, pp. 167–179, 2007. [CrossRef] [Google Scholar] [Publisher Link]

[12] Thomas Riegler et al., "Nanoscale Relationships between Uranium and Carbonaceous Material in Alteration Halos Around Unconformity-Related Uranium Deposits of the Kiggavik Camp, Paleoproterozoic Thelon Basin, Nunavut, Canada," *Ore Geology Reviews*, vol. 79, pp. 382-391, 2016. [CrossRef] [Google Scholar] [Publisher Link]

[13] Abdou Dodo Bohari1, Moussa Harouna, and Ali Mosaad**,** "Geochemistry of Sandstone Type Uranium Deposit in Tarat Formation from Tim-Mersoi Basin in Northern Niger (West Africa): Implication on Provenance, Paleo-Redox and Tectonic Setting," *Journal of Geoscience and Environment Protection*, vol. 6, no. 8, 2018. [CrossRef] [Google Scholar] [Publisher Link]

[14] P Bowden et al., "Uranium in the Niger-Nigeria Younger Granite Province," *Mineralogical Magazine*, vol. 44, no. 336, pp. 379–389, 2018. [CrossRef] [Google Scholar] [Publisher Link]

[15] D. P. Nicholls et al., "Polarity Determination of Zinc Oxide Nanorods by Defocused Convergent-Beam Electron Diffraction," *Philosophical Magazine Letters*, vol. 87, no. 6, pp. 417-421, 2007. [CrossRef] [Google Scholar] [Publisher Link]

[16] Idris Mohammed Jega, Alexis J. Comber, and Nicholas J. Tate, "A Comparison of Methods for Spatial Interpolation across Different Spatial Scales," *SSRG International Journal of Geoinformatics and Geological Science*, vol. 4, no. 2, pp. 12-22, 2017. [CrossRef] [Google Scholar] [Publisher Link]

[17] J Navez et al., "The Palaeoproterozoic Tchilit Exotic Terrane (Air, Niger) within the Pan-African Collage of the Tuareg Shield," *Journal of the Geological Society of London*, vol. 156, pp. 247–259, 1999. [CrossRef] [Google Scholar] [Publisher Link]

[18] Nguo Sylvestre Kanouo et al., "Trace and REEs Geochemistry, A Tool to Study Mudrocks and Quaternary Deposits Found in Babouri-Figuil Intracontinental Basin (North Cameroon): Provenance, Depositional Conditions, and Paleoclimate," *SSRG International Journal of Geoinformatics and Geological Science*, vol. 8, no. 2, pp. 67-88, 2021. [Crossref] [Google Scholar] [Publisher Link]

[19] El Hamet, Mai Ousman, "Geological analysis and petrographic training Tarata in careers (Upper Paleozoic)-test paleoclimatic interpretation in the light of the glacial episode devono-carboniferous (Arlit region, northern Niger); Analyse Geologique et petrographique de la formation de tarat dans les carrieres (paleozoique superieur) -essai d'interpretation paleoclimatique a la lumiere de l'episode glaciaire devono-carbonifere(region d'arlit-Niger septentrional)," 1983. [Google Scholar] [Publisher Link]

[20] Moussa Konaté et al., "Structuration Extensive Et Transtensive Au Devono-Dinantien Du Bassin De Tim Mersoï (Bordure Occidentale De L'aïr, Nord Niger0," *Annales de l'Université de Ouagadougou*, vol. 5, pp. 1–32, 2007. [Google Scholar] [Publisher Link]

[21] D. Salze, O. Belcourt, and M. Harouna, "The First Stage in the Formation of the Uranium Deposit of Arlit, Niger : Role of a New non-Continental Organic Matter," *Ore Geology Reviews*, vol. 102, pp. 604–617, 2018. [CrossRef] [Google Scholar] [Publisher Link]

[22] S.S. Adams et al., "Interpretation of Postdepositional Processes Related to the Formation and Destruction of the Jackpile-Paguate Uranium Deposit, Northwest New Mexico," *Economic Geology*, vol. 73, no. 8, pp. 1635–1654, 1978. [CrossRef] [Google Scholar] [Publisher Link]

[23] C. Amrhein, P.A.Mosher, A.D. Brown, "The Effects of Redox on Mo, U, B, V and as Solubility in Evaporation Pond Soil," S*oil Science*, vol. 155, no. 4, pp. 249-255, 1993. [CrossRef] [Google Scholar] [Publisher Link]

[24] Fayek, M, *Uranium ore deposits: A review. Mineralogical Association of Canada Short Course Series*, Uranium: cradle to grave, vol. 43, pp. 121-147, 2013.[Google Scholar]

[25] Pooja Sharma, Arun Kumar Shandilya, and Neeraj Srivastave, "Geological Settings, Mineralization and Genesis of Iron Ore Deposit at Pur-Banera Belt of District Bhilwara, Rajasthan (India)," *SSRG International Journal of Geoinformatics and Geological Science*, vol. 7, no. 2, pp. 47-54, 2020. [CrossRef] [Publisher Link]

[26] Fengjun Nie et al., "Genetic Models and Exploration Implication of the Paleochannel Sandstone-Type Uranium Deposits in the Erlian Basin, North China- A Review And Comparative Study," *Ore Geology Reviews*, vol. 127, 2020. [CrossRef] [Google Scholar] [Publisher Link]

[27] Maurice Pagel et al.**,** *Uranium Deposits in the Arlit Area (Niger*). Mineral Deposit Research: Meeting the Global Challenge, Springer, pp. 303-305, 2005. [CrossRef] [Google Scholar] [Publisher Link]

[28] Michał Rakocinski et al., "Redox Conditions, Productivity, and Volcanic Input During Deposition of Uppermost Jurassic and Lower Cretaceous Organic-Rich Siltstones in Spitsbergen, Norway," *Cretaceous Research*, vol. 89, pp. 126–147, 2018. [CrossRef] [Google Scholar] [Publisher Link]

[29] David Salze, "Study of Interactions Between Uranium and Organic Compounds in Hydrothermal Systems," *Universite Henri Poincare – Nancy*, 2008. [Google Scholar] [Publisher Link]

[30] C.A. Kogbe, **"**Stratigraphy and Tectonic History of the Iullemeden Basin in West Africa," *South African Journal of Geology*, vol. 94, pp. 19-31, 1991. [Google Scholar] [Publisher Link]

[31] Gerbeaud, O, Evolution structurale du bassin de Tim Mersoï: Le rôle des déformations de la couverture sédimentaire sur la mise en place des gisements uranifères du secteur d'Arlit (Niger) ,Thèse de Doctorat, Orsay, France: Université de Paris Sud, 2006. [Google Scholar] [Publisher Link]